

1-2023

Precise Zircon U-Pb Dating of the Mesoproterozoic Gawler Large Igneous Province, South Australia

Elizabeth A. Jagodzinski
Geological Survey of South Australia

Anthony J. Reid
Geological Survey of South Australia

James L. Crowley
Boise State University

Claire E. Wade
Geological Survey of South Australia

Stacey Curtis
Geological Survey of South Australia

Publication Information

Jagodzinski, Elizabeth A.; Reid, Anthony J.; Crowley, James L.; Wade, Claire E.; and Curtis, Stacey. (2023). "Precise Zircon U-Pb Dating of the Mesoproterozoic Gawler Large Igneous Province, South Australia". *Results in Geochemistry*, 10, 100020. <https://doi.org/10.1016/j.ringeo.2022.100020>



Precise zircon U-Pb dating of the Mesoproterozoic Gawler large igneous province, South Australia

Elizabeth A. Jagodzinski^{a,*}, Anthony J. Reid^{a,b}, James L. Crowley^c, Claire E. Wade^a, Stacey Curtis^a

^a Geological Survey of South Australia, Department of State Development, 101 Grenfell Street, Adelaide, SA 5001, Australia

^b Department of Earth Sciences, University of Adelaide, Adelaide, South Australia 5005, Australia

^c Department of Geosciences, Boise State University, 1910 University Drive, Boise, ID 83725-1535, USA

ARTICLE INFO

Keywords:

Mesoproterozoic silicic large igneous province
CA-TIMS geochronology
Gawler range volcanics
Benagerie volcanic suite
Continental flood rhyolites
Mantle plume

ABSTRACT

The Mesoproterozoic Gawler Range Volcanics and Benagerie Volcanic Suite of the Gawler Craton and Curnamona Province, South Australia, together with associated intrusive magmatism, define an intracontinental, subaerial large igneous province (LIP) preserving an estimated 110 000 km³ of volcanic rock, which hosts one of the world's largest orebodies, the Fe oxide-Cu-Au-U deposit at Olympic Dam, and numerous other related Cu-Au deposits. New high-precision Chemical Abrasion Isotope Dilution Thermal Ionization Mass Spectrometry (CA-TIMS) U-Pb dates on volcanic zircons allow for regional correlations between stratigraphic units of the GRV and BVS, and an understanding of how magmatic styles, temperatures, composition and mantle source input evolve over the duration of the LIP. The new dates indicate that the entire volcanic province erupted over a geologically short time interval of less than 10 million years, from c. 1595 to 1586 Ma, culminating in a widespread, voluminous flood rhyolite province that erupted in less than 1.5 million years, and most likely in 260,000 years or less. This follows a pattern of volcanism that is similar in duration and volume to mafic and bimodal continental LIPs, of which the mafic-dominated Phanerozoic continental flood basalt provinces are the more common end member.

Introduction

Large igneous provinces (LIPs) are one of the most striking manifestations of magmatic activity on Earth. Such provinces typically comprise volcanic rocks with eruptive volumes estimated in the hundreds of thousands to millions of cubic kilometers (Ernst, 2014 and references therein), the eruption of which has been linked to mass extinction events (Schoene et al., 2010), supercontinental assembly and disaggregation (Ernst et al., 2013) and formation of some of the world's greatest ore deposits (Ernst & Jowitt, 2013). South Australia preserves one of the relatively rare examples of a LIP dominated by silicic volcanic rocks (Bryan & Ernst, 2008; Bryan & Ferrari, 2013; Pankhurst et al., 2011a, 2011b). The early Mesoproterozoic Gawler LIP extends from the central Gawler Craton into the once adjacent central-western Curnamona Province (McPhie et al., 2008; Pankhurst et al., 2011b; Wade et al., 2012) (Fig. 1). In the Gawler Craton this LIP is manifest as the Gawler Range Volcanics (GRV), the stratigraphy of which has been developed based on mapping and geochemical characterisation (Allen

et al., 2008; Blissett et al., 1993) (Fig. 2). The GRV are subdivided into a lower and upper sequence, representing different styles of eruptive volcanism. In the Curnamona Province, the Benagerie Volcanic Suite (BVS) is known only from drill holes (Wade et al., 2011), so the stratigraphy of the succession is not as well defined.

Though the Gawler Craton and Curnamona Province are now separated by a Neoproterozoic rift sequence (the Adelaide Rift Complex, Lloyd et al., 2020; Sprigg, 1952), they were formerly joined in the Mesoproterozoic, forming the Proterozoic entity known as the South Australian Craton (Myers et al., 1996). Palaeo-Mesoproterozoic basement inliers of the Barossa Complex lie within the Adelaide Rift Complex, linking these two cratonic elements (Jagodzinski et al., 2020; Szpunar et al., 2007) (Fig. 1). Their volcanic provinces, together with co-genetic intrusive rocks (the Hiltaba Suite in the Gawler Craton and Ninnerie Supersuite in the Curnamona Province) are associated with the formation of the Olympic Dam Cu-Au-U deposit and a host of other Cu-Au, Au and Ag-Pb mineral deposits, and are thus of major economic significance (Johnson & Cross, 1995; Reid, 2019; Skirrow, 2003;

* Corresponding author.

E-mail address: liz.jagodzinski@sa.gov.au (E.A. Jagodzinski).

<https://doi.org/10.1016/j.ringeo.2022.100020>

Available online 5 December 2022

2666-2779/Crown Copyright © 2022 Published by Elsevier B.V. This is an open access article under the CC BY-NC-ND license (<http://creativecommons.org/licenses/by-nc-nd/4.0/>).

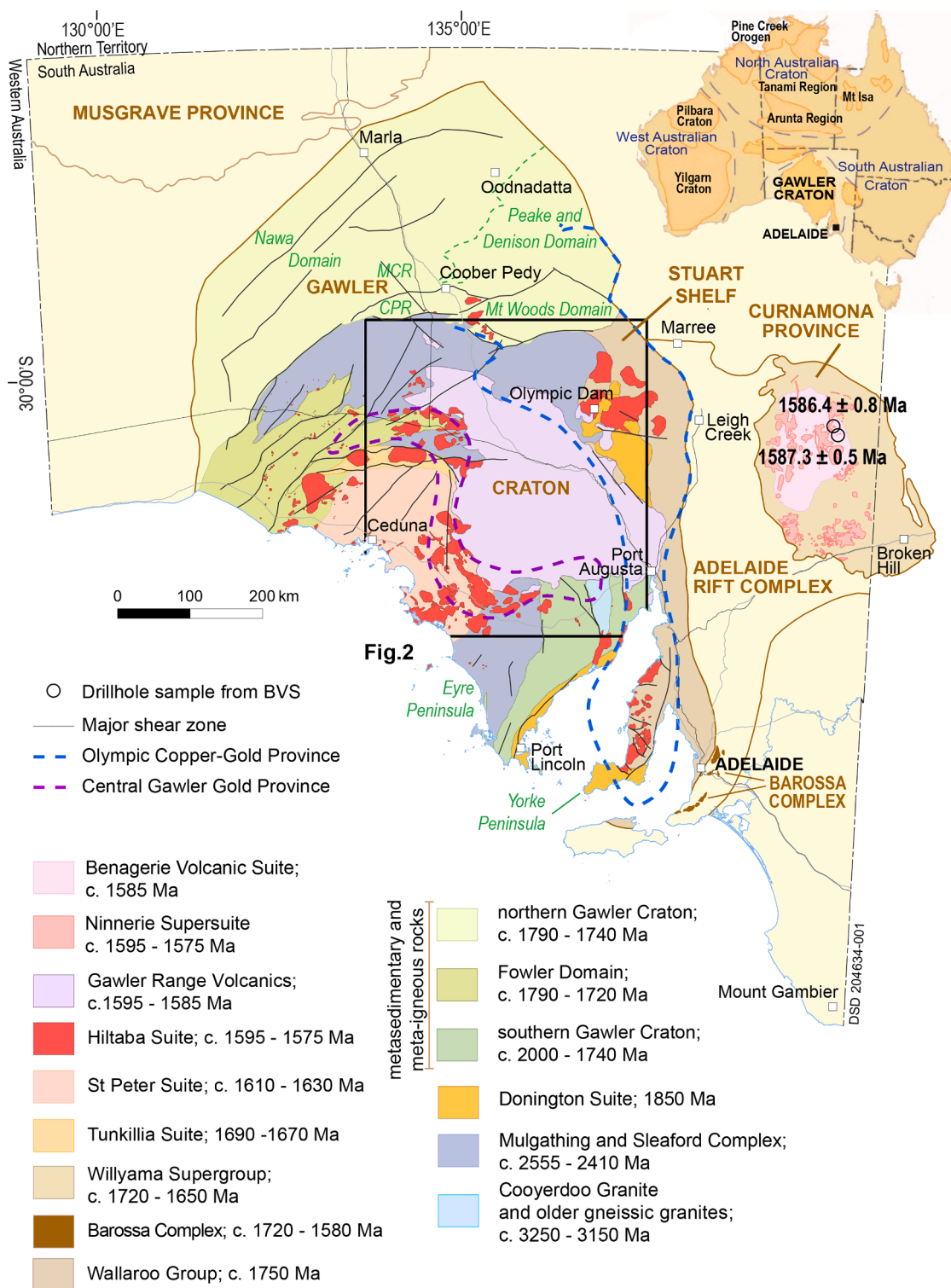


Fig. 1. The main lithostratigraphic units of the Gawler Craton and Curnamona Province, South Australia, interpreted from surface observation and geophysical data. Inset shows the location of the Gawler Craton and Curnamona Province in the context of major Archean and Proterozoic terranes of Australia. Also indicated are the metallogenic provinces associated with this large igneous province, the Olympic Cu-Au Province and the Central Gawler Gold Province. The locations of the two samples from the BVS are plotted labelled with their ages. GRV samples are similarly plotted in Fig. 2.

Skirrow et al., 2007; Tiddy & Giles, 2020). Consequently, this Mesoproterozoic thermal event encompassing widespread magmatism and associated metamorphism and mineralisation, has been dated more than any other time slice of South Australia’s geological history (Table 1).

This study provides a unique example of temporally constrained mafic and silicic volcanism in a stratigraphically well-defined

Proterozoic LIP. It documents newly acquired, high-precision CA-TIMS dates from samples selected to embody the full temporal and spatial range of the GRV and BVS, with representation from each of the recognised volcanic successions. New high-precision dates for the volcanic rocks (this study) and co-magmatic intrusions of the Hiltaba Suite (Cherry et al., 2018; Courtney-Davies et al., 2020; Jagodzinski et al.,

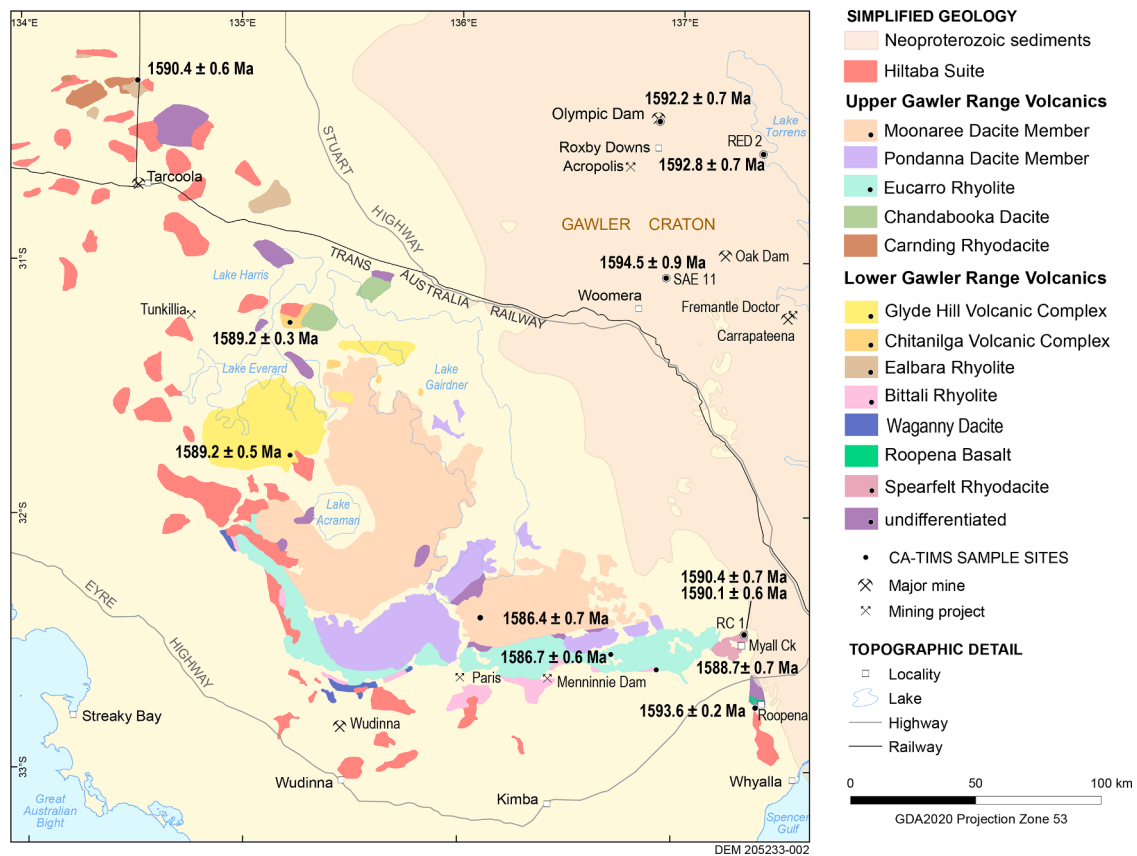


Fig. 2. Simplified outcrop geological map of the GRV region. Samples analysed in this study are indicated and labelled with their ages, as are the major stratigraphic subdivisions of the GRV along with major mines and mineral deposits.

2021; McPhie et al., 2020; Reid et al., 2021) are used to assess the validity of spatial and temporal trends observed in a larger pre-existing data set of lower-precision dates. They also allow for the temporal correlation of spatially separate volcanic sequences, determining the duration of volcanism and magmatism, the age span of the lower and upper GRV and the age of the boundary between them, which marks a distinctive change in style of volcanism in the province. The revised stratigraphy and regional correlation between units of the GRV also provide an opportunity to study the temporal, geochemical and isotopic evolution of the Gawler LIP, with respect to mantle evolution and crustal melting behaviour above a plume. This is explored in a companion paper (Wade et al., 2022).

Geological setting

The GRV and co-magmatic plutons of the Hiltaba Suite outcrop over c. 25 000 km² of the central Gawler Craton (Fig. 2) and extend beneath younger formations of the Stuart Shelf to the northeast, giving a total extent of 90 000 km², with an estimated volume of c. 70 000 km³ for the GRV and 30 000 km³ for the Hiltaba Suite (McPhie et al., 2008). An additional 18 000 km² of BVS in the once-adjacent Curnamona Province means an estimated c. 110 000 km³ of magma was erupted or emplaced during formation of the Gawler LIP (Wade et al., 2012). The volcanic rocks were emplaced in a subaerial, intracontinental setting. In the Gawler Craton, the GRV overlie a thick, c. 3250 – 1610 Ma crustal sequence, which records multiple episodes of crustal growth and reworking (Reid and Hand, 2012 and references therein) (Fig. 3). Deformed Mesoarchaean granites and granite gneisses (c. 3250 – 3150 Ma) and Palaeoproterozoic metamorphic complexes (c. 2520–2420 Ma) underlie craton-wide supracrustal volcano-sedimentary successions (c. 2000–1650 Ma). Sedimentation was largely terminated by basin

inversion associated with the c. 1730–1690 Ma Kimban Orogeny, and subsequent events were predominantly igneous with episodes of magmatism at c. 1690 – 1670 Ma (Tunkillia Suite) and c. 1635 – 1605 Ma (St Peter Suite), culminating in the most volumetrically and economically significant of these at c. 1595–1575 Ma (GRV and Hiltaba Suite). In the Curnamona Province supracrustal units of the c. 1720–1650 Ma Will-yama Supergroup form a basement to the BVS and co-eval granites of the Ninnerie Supersuite (Conor and Preiss, 2008; Stevens et al., 1988).

Although themselves undeformed, emplacement of the volcanic and plutonic rocks of the Gawler LIP in the upper crust was broadly synchronous with granulite facies metamorphism, deformation and melting of the mid-lower crust, which is preserved around the margins of the Gawler Craton (Mt Woods Domain, Coober Pedy Ridge, Mabel Creek Ridge and Yorke Peninsula), and in the Barossa Complex and Curnamona Province. In the Gawler Craton this orogenic event is broadly referred to as the Kararan Orogeny (c. 1595–1575 Ma metamorphism, with a younger overprint of ages ranging down to c. 1530 Ma), and in the Barossa Complex and Curnamona Province as the Olarian Orogeny (c. 1610–1580 Ma, Forbes et al., 2005; Page et al., 2005).

The GRV is subdivided into a lower sequence of gently to moderately dipping older units and an upper sequence of extensive, flat-lying younger units (Blissett et al., 1993). The first expression of volcanism, represented by the lower GRV, comprises at least six, widely separated outcropping successions at Tarcoola (Daly, 1985), Chitanilga Volcanic Complex southeast of Lake Harris (Blissett, 1975; Branch, 1978) and Glyde Hill Volcanic Complex at Lake Everard (Blissett, 1975; Giles, 1988) in the northwest, and Roopena (McAvaney & Wade, 2015), Myall Creek (Simpson, 2017) and Menninnie Dam (Roache et al., 2000) in the southeast (Fig. 2). The lower GRV also occurs within inliers beneath the upper GRV and beneath the Neoproterozoic to Phanerozoic cover of the Stuart Shelf to the east, at Olympic Dam and surrounding prospects

Table 1

Summary of published dates for the Gawler Range Volcanics (GRV) and Benagerie Volcanic Suite (BVS). OD = Olympic Dam, BCF = bedded clastic facies, ODBC = Olympic Dam Breccia Complex, RDG = Roxby Downs Granite. Only CA-TIMS dates are listed for the Hiltaba Suite. Table D1 of the supplementary dataset (Electronic Appendix 1) is a comprehensive list of all magmatic ages for the Gawler LIP with sample numbers, locations and references.

Sample Identifier Lithology/Location/DDH	Age Ma	± Ma	Data Source
lower GRV - OD and surrounding prospects			
BCF, OD	1597	8	11
clast in ODBC, RD647	1594.6	0.7	3
clast in ODBC, MJ54WEST	1594.3	0.5	2
dyke, RD1408	1594	4	8
dyke, RU45-4425	1594	4	8
clast in ODBC, SSH255	1594.0	0.6	2
clast in ODBC, RD1624	1593.7	0.5	2
rhyolite, ACD2, Acropolis	1593.2	0.7	12
dyke, ACD19, Acropolis	1593.0	0.6	12
volcanic breccia, RD647, OD	1593	6	8
dyke, RU52-5476, OD	1593	5	8
volcanic breccia, RD32, OD	1592	8	11
BCF, RU38-2625, OD	1592	4	8
dyke, RU3-739, OD	1592	6	8
quartz latite, ACD5, Acropolis	1591	10	4
BCF, RD3449, OD	1590.4	0.8	2
BCF, OD	1589.9	0.9	2
porphyry, SAE11, Emmie Bluff	1583	12	7
ACD5, Acropolis	1576	22	13
Hiltaba Suite, OD and surrounding prospects			
RDG, RD2786A 1516 m, OD	1596.0	0.9	3
RDG, RD2786A 1850 m, OD	1594.5	1.7	3
ACD7 599 m, Acropolis	1594.0	0.6	12
RDG, RD2786A 1830 m, OD	1593.4	1.1	3
RDG, RD2786A 1810 m, OD	1593.3	0.5	3
RDG, RD2499 814.1 m, OD	1593.3	0.7	2
RDG, RD2488 681.9 m, OD	1593.1	0.6	2
RDG, RD575 531 m, OD	1593.1	0.6	2
RDG, RD2499 529.7 m, OD	1593.0	0.5	2
RDG, RD2284 352.8 m, OD	1592.7	1.3	2
BRD1 816–817 m	1592.6	0.7	9
Blanche1 1563.1-1564.6 m	1591.8	0.7	9
lower GRV - Gawler Ranges and surrounds			
dyke, MD003, Menninie Dam	1604	11	7
dyke, PLAC003, Peterlumbo	1597	14	14
dyke, MD003, Menninie Dam	1594	11	7
Childera Dacite, Glyde Hill	1592	17	1
Wanganny Dacite, Kondoolka	1591	3	6
Ealbara Rhyolite, Tarcoola	1589	16	1
Fresh Well Fm, DDH6, Roopena	1587	15	10
granophyre, Cultana Complex	1584	3	1
upper GRV, Gawler Ranges			
Moonarie Dacite Member	1598	10	16
Moonarie Dacite Member	1592	3	5
Hiltaba Suite, Central Gawler Craton			
Cooladding Granite, Tarcoola	1586.5	0.6	9
Hiltaba Suite, Yorke Peninsula			
Tickera Granite, Point Riley	1584.2	0.8	15
Tickera Granite, Point Riley	1582.7	1.4	15
Tickera Granite, Point Riley	1579.1	0.8	15
gabbro, CURD2	1580.2	0.4	9
Hiltaba Suite, Fowler Domain			
NDR13 94.5–94.7 m	1579.4	1.6	9
BVS, Curnamona Province			
rhyolite, Frome13	1587	6	17
rhyolite, Culbertal	1584	6	17
rhyolite, Mudguard1	1584	5	17
rhyolite, Mudguard1	1581	4	6

Data sources and dating methods: 1. Blissett et al. (1993) ID-TIMS (multi-zircon isotope dilution thermal ionization mass spectrometry); 2. Chery et al. (2018) CA-TIMS; 3. Courtney-Davies et al. (2020) CA-TIMS; 4. Creaser & Cooper (1993) ID-TIMS; 5. Fanning et al. (2007) ID-TIMS; 6. Fanning et al. (1988) SHRIMP; 7. Fanning et al. (2007) SHRIMP; 8. Jagodzinski (2014) SHRIMP; 9. Jagodzinski et al. (2021) CA-TIMS; 10. Johnson (1993) SHRIMP; 11. Johnson & Cross (1995) SHRIMP; 12. McPhie et al. (2020) CA-TIMS; 13. Mortimer et al. (1988) ID-TIMS; 14. Reid & Jagodzinski (2012) SHRIMP; 15. Reid et al. (2021) CA-TIMS; 16. Reid et al. (2006) La-ICPMS (Laser Ablation Inductively Coupled Plasma Mass

Spectrometry); 17. Wade et al. (2012) SHRIMP. CA-TIMS dates from Chery et al. (2018) and McPhie et al. (2020) have been recalculated using a $^{238}\text{U}/^{235}\text{U}$ value of 137.8185 (Hiess et al., 2012) to compare with dates in this study, and therefore differ from the original publications by ~ 0.84 Ma.

(Belperio et al., 2007; Bull et al., 2015; McPhie et al., 2016, 2020). The lower GRV successions consist of small- to moderate-volume effusive and explosive eruptions from numerous discrete volcanic centres tapping small magma chambers. These formed lithologically and compositionally variable successions up to 3 km thick of porphyritic dacite and rhyolite lavas, minor ignimbrites and volcanoclastic rocks, accompanied by mafic volcanism. Coherent geochemical and isotopic trends between basalts and rhyolites indicate a relationship through crystal fractionation, with some crustal assimilation in the silicic units (Chapman et al., 2019; Creaser, 1995; Giles, 1988; Stewart 1994; Wade et al., 2022). Thin packages of sedimentary rocks, commonly containing resedimented pyroclasts, intercalate locally with the volcanic rocks with limited lateral extent (Allen et al., 2008). Relicts of larger syn-sedimentary basins are preserved in the eastern Gawler Craton at Olympic Dam (McPhie et al., 2016), Prominent Hill (Belperio et al., 2007; Bull et al., 2015), Myall Creek (Simpson, 2017) and Roopena (Curtis et al., 2018).

The upper GRV consists of voluminous, thick (c. 300 m), regionally extensive, crystal rich (15–40%) rhyolitic and dacitic sheet lavas forming three stratigraphic units; the Eucarro Rhyolite, and the Pondanna Dacite and Moonaree Dacite members of the Yardea Dacite (Allen & McPhie, 2002; Allen et al., 2008; Garner & McPhie, 1999; Morrow & McPhie, 2000). Each represents about 1000 – 4000 km³ of magma, making them at least an order of magnitude larger than small- to moderate-sized lavas in the lower GRV (Allen et al., 2003, 2008). In contrast to the lower GRV, they have no associated mafic component apart from rare mafic igneous clasts up to 5 cm scattered throughout the flows. The flows have simple cooling profiles consistent with cooling and degassing as single effusive emplacement units (Allen & McPhie, 2002; Allen et al., 2003). Basal sections are commonly black, and flow banded, with a crypto- to microcrystalline groundmass indicating that they were originally glassy and cooled rapidly. The middle red or pink facies have well-developed columnar jointing and groundmass textures that range from granophyric in the interior to spherulitic and micropoikilitic towards the margins, consistent with the interior undergoing slower cooling. Flow tops are amygdaloidal or autobrecciated, where preserved. Extensive outflow of the crystal-rich lavas was enabled by their high temperatures (950 – 1100 °C) and high F concentrations, which would have lowered viscosity (Agangi et al., 2012; Creaser & White, 1991; Pankhurst et al., 2011b; Stewart, 1994), and their high eruption volumes producing thick flows likely to be well insulated by outer crusts (Allen et al., 2003; Manley, 1992). The upper GRV lavas are geochemically and isotopically homogenous, reflecting a change in the plumbing system from small, isolated magma chambers to large magma reservoirs of batholithic proportions (Allen et al., 2008; Stewart 1994; Wade et al., 2022). Vent sources for the upper GRV lavas have yet to be identified. Allen & McPhie (2002) suggest eruption from multiple vents along a fissure would better account for widespread outflow than a point source, whereas Pankhurst (2011b) postulate a central cluster of feeder vents producing large-scale lobate flow patterns visible in geophysical images. The Eucarro Rhyolite and overlying Pondanna Dacite Member are separated by a thin (30 – 100 m), regionally extensive marker horizons of pyroclastic, volcanoclastic and volcanogenic sedimentary rocks of the Mount Friday Formation, Mount Double Ignimbrite and Nonning Sandstone. Locally, the 'Yartoo volcanoclastics', comprising a clast-bearing volcanic mudstone or matrix-supported volcanic breccia/conglomerate, separate the Pondanna and Moonaree Dacite (Werner et al., 2017).

The Benagerie Volcanic Suite (Wade et al., 2012) extends over about 8 000 km² beneath widespread Phanerozoic sedimentary cover in the Moorowie Sub-basin and Frome Embayment in the Benagerie Ridge area of the Curnamona Province and is known only from drill holes. It

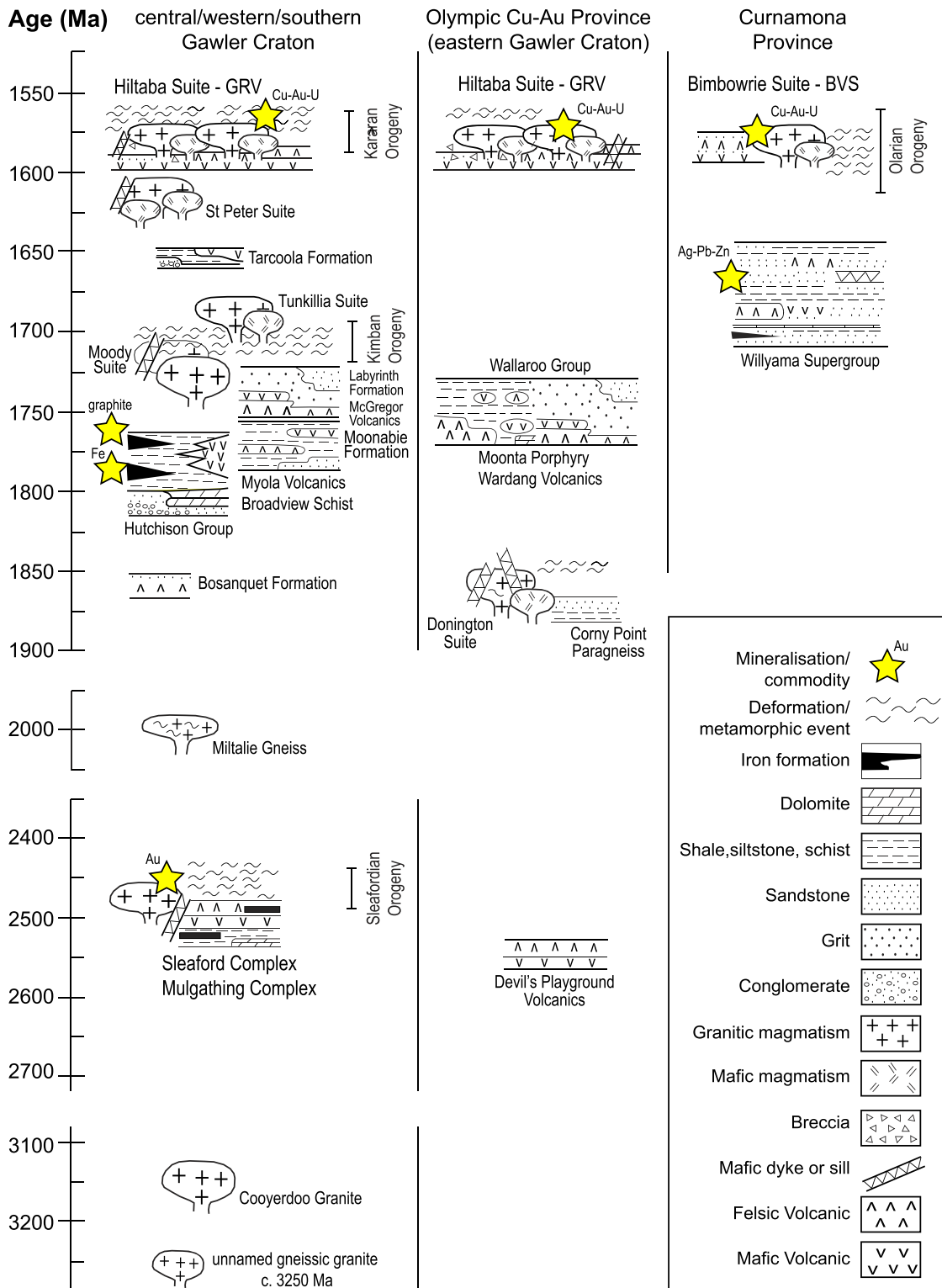


Fig. 3. Simplified time-space diagram illustrating the main lithotectonic elements of the Gawler Craton and Curnamona Province. This figure highlights lithotectonic differences between the eastern and western Gawler Craton, with the region of the Olympic Dam Cu-Au Province broadly equivalent to the eastern Gawler Craton. For discussion see Reid & Hand (2012).

comprises unnamed mafic volcanics which are probably equivalent to the lower GRV, and more extensive rhyolite lavas, the Finlay Dam Rhyolite and Lake Elder Rhyodacite, which have been correlated with the upper GRV (Flint et al., 1993; Giles & Teale, 1979; Wade et al., 2012).

Analytical method

U-Pb dates were obtained by the chemical abrasion isotope dilution thermal ionization mass spectrometry (CA-TIMS) method from analyses of single zircon grains. Analyses were conducted at the Isotope Geology Laboratory at Boise State University, Idaho. A detailed description of the

Table 2Summary of the stratigraphy and locations of samples dated during this study, together with their weighted mean $^{207}\text{Pb}/^{206}\text{Pb}$ ages.

#	Sample	Lithology and Location	GDA 2000			Age (Ma)	\pm c95%	MSWD	pof	n	n _t
			Easting	Northing	MGA Zone						
lower GRV - Olympic Dam and surrounds											
1	2131354	volcaniclastic sandstone, SAE11, 970.7–971.35 m, Emmie Bluff	684880	6560673	53	1594.53	0.88	0.83	0.51	5	10
2	2131365	dacite, RED 2 363.3–369 m, Red Dam	727057	6615051	53	1592.79	0.71	1.67	0.14	6	6
3	2000-366166	sericitised dyke, RU45–4425 100.5–102.2 m, Olympic Dam	680209	6631024	53	1592.21	0.66	0.66	0.65	6	8
lower GRV - south-eastern margin of the Gawler Ranges											
4	2017742	porphyritic lava, Angle Dam Dacite, Roopena	723319	6374760	53	1593.61	0.19	0.68	0.64	6	6
5	2116682	lava, Spearfelt Rhyodacite, RC1 15.65–16.77m	718925	6405396	53	1590.35	0.65	0.68	0.64	6	6
6	2116683	lava, map unit Ma15, RC1 118.14–119.1m	718925	6405396	53	1590.13	0.62	0.52	0.76	6	8
7	2018616	lava, Bittali Rhyolite	681774	6390462	53	1588.47	0.66	0.26	0.94	6	6
lower GRV - north-western margin of the Gawler Ranges											
8	2016125	ignimbrite, Ealbara Rhyolite, Birthday Quarry, Tarcoola	454533	6647511	53	1590.35	0.64	0.31	0.91	6	6
9	2746487	ignimbrite, Chitanilga Volcanic Complex, Kokatha	519635	6544209	53	1589.19	0.32	1.78	0.10	7	8
10	2721839	lava, Mangaroonah Dacite, Glyde Hill Volcanic Complex	519800	6485620	53	1589.19	0.48	1.52	0.19	5	5
upper GRV - Gawler Ranges											
11	1998158	lava, Eucarro Rhyolite, south-eastern Gawler Ranges	660499	6397579	53	1586.65	0.64	1.06	0.38	6	6
12	1998160	lava, Moonaree Dacite Member, central Gawler Ranges	603746	6413021	53	1586.39	0.66	0.56	0.73	6	6
BVS - Curnamona Province											
13	2049215	rhyolite porphyry, Finlay Dam Rhyolite, CU 1 435.55–439m	444351	6601735	54	1587.31	0.51	0.55	0.80	8	8
14	2049213	rhyolite porphyry, Finlay Dam Rhyolite, BRD013 466–484m	437448	6613971	54	1586.44	0.78	1.60	0.16	6	6

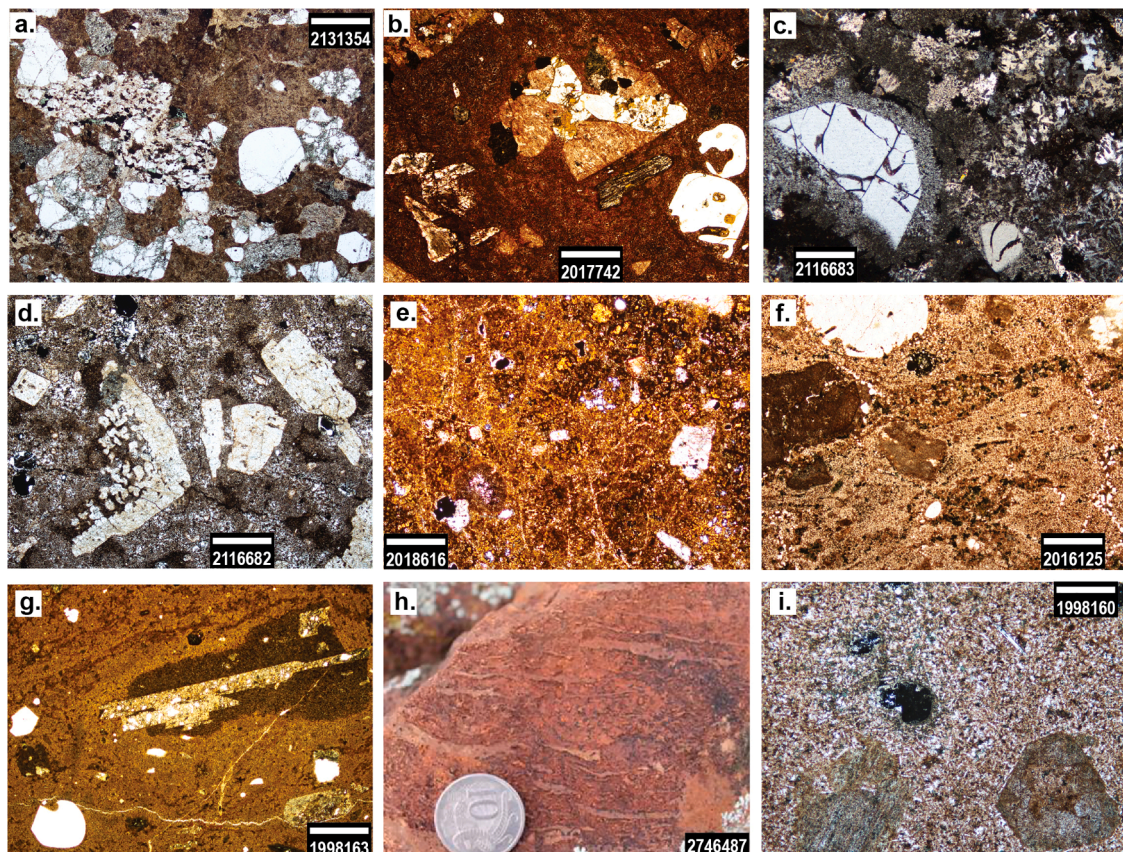
NB: errors on the dates are quoted at the 95% confidence level (\pm c95%) = $\tau\sigma$ for MSWD \leq 1.0, $\tau\sigma\sqrt{\text{MSWD}}$ for MSWD > 1.0.

Fig. 4. Photomicrographs and outcrop photos highlighting some of the different textural features of the GRV. All samples are described in detail in section S2 of the supplementary text. Plane polarised light (a,b,d,e,f,g), cross polars (c,i). Scalebar is 1 mm. **a.** The clastic texture of 2131354, SAE 11, Emmie Bluff, with abundant lithic clasts. The brown matted areas are altered feldspars. **b.** Feldspar-leucoxene-chlorite (replacing biotite) glomerocryst and magmatically-resorbed quartz phenocrysts, Angle Dam Dacite, Roopena (2017742). **c.** Quartz phenocrysts mantled by optically continuous groundmass quartz, with closely packed patches of poikilitic quartz enclosing small K-feldspar crystals in the groundmass, Unit Ma15, RC1, Myall Creek (2116683). **d.** Resorbed spongy plagioclase phenocryst in a micro-poikilitic groundmass, Spearfelt Rhyodacite, RC1, Myall Creek (2116682). **e.** Perlite fractures within a haematite-altered groundmass, Bittali Rhyolite (2018616). **f.** Fiammé wrapping phenocrysts and forming a weak eutaxitic texture, Ealbara Rhyolite, Tarcoola (2016125). **g.** Plagioclase phenocryst aligned with flow banding, Mangaroonah Dacite, Glyde Hill Volcanic Complex (1998163). **h.** Compaction of fiammé forming a moderate eutaxitic texture in ignimbrite Chitanilga Volcanic Complex (2746487). **i.** Abundant plagioclase microlites (quench crystals) in a finely microcrystalline groundmass, Moonaree Dacite Member, upper GRV (1998160).

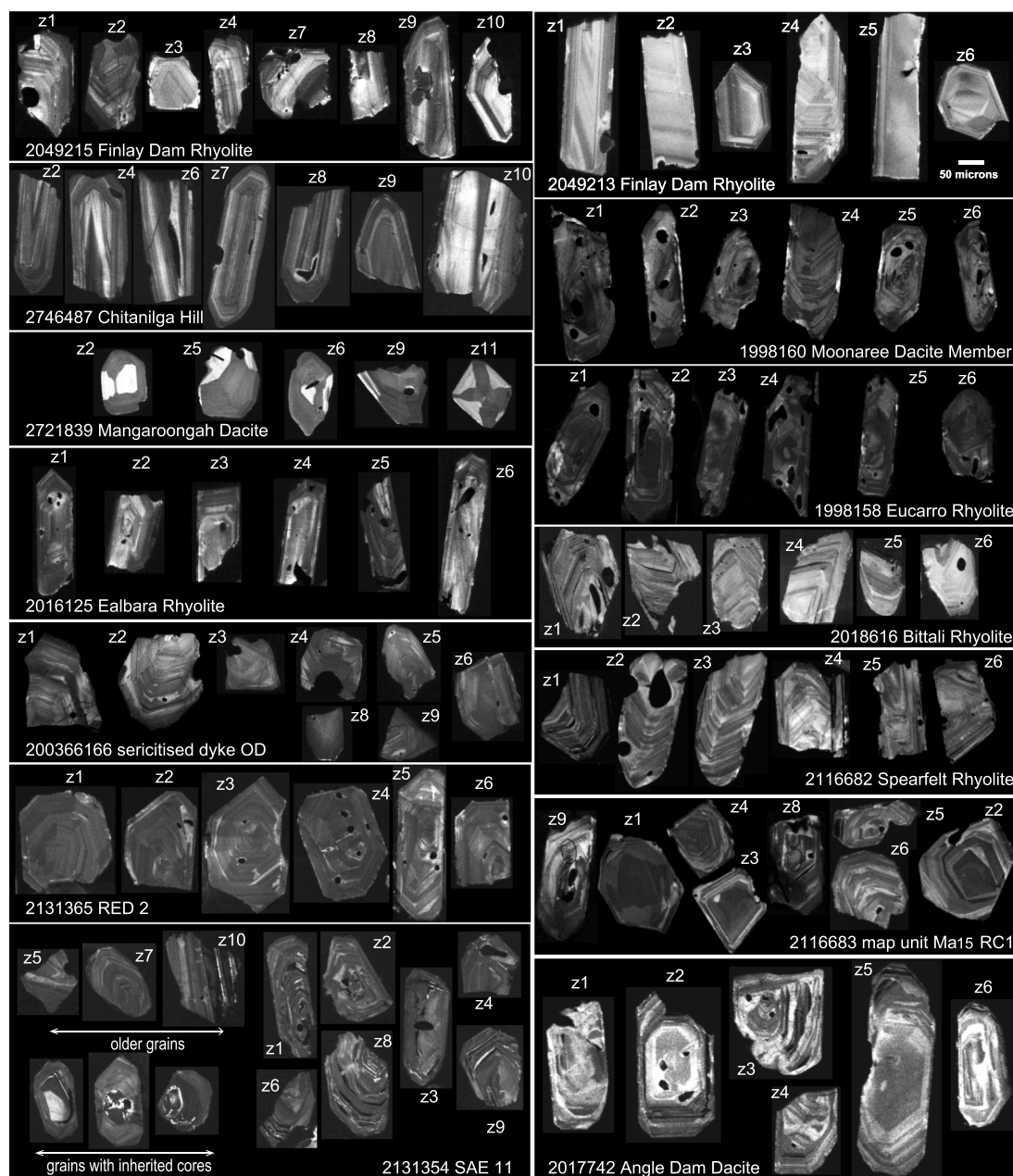


Fig. 5. Cathodoluminescence (CL) images of zircon used for CA-TIMS analysis, collected with a scanning electron microscope at Boise State University. Grains labels z1, z2, etc. correspond to the analysis number in the CA-TIMS dataset in the supplement (Table D2). Brightness of grains can be directly compared within samples, but not between samples.

method is provided in section S1 of the supplementary text, and data are presented in Table D2 of the supplementary dataset. Grains were selected for dating from the 14 samples listed in Table 2. The samples were chosen to represent the full temporal and spatial extent of the lower and upper GRV and BVS (Figs. 1, 2). The volcanic facies selected for dating are predominantly coherent rhyolite, rhyodacite and dacite lavas characterised by an evenly porphyritic texture and euhedral/subhedral phenocrysts within an originally glassy to devitrified groundmass, but also include ignimbrites, one dyke and one volcanoclastic sandstone (Table 2, Fig. 4). For some samples collected from drill holes (RED 2, CU1, BRD 013), the absence of upper and lower contacts makes it difficult to distinguish whether the volcanic unit was emplaced as a lava flow or a high-level sill. The samples are described in more detail in section S2 of the supplementary text. Cathodoluminescence (CL) images for the zircon grains are shown in Fig. 5.

Between five grains and ten grains were analysed from each sample. Isoplot 3.75 (Ludwig, 2012) is used to calculate weighted mean $^{207}\text{Pb}/^{206}\text{Pb}$ dates from equivalent dates (probability of fit > 0.05), which are used to interpret igneous crystallisation ages. The $^{207}\text{Pb}/^{206}\text{Pb}$ dates are used rather than $^{206}\text{Pb}/^{238}\text{U}$ dates due to some $^{206}\text{Pb}/^{238}\text{U}$ dates being slightly younger, presumably due to some incipient Pb loss, which is common for rocks of Mesoproterozoic age. The reported dates utilise the U decay constants recommended by Jaffey et al. (1971), and $^{238}\text{U}/^{235}\text{U}$ of 137.818 (2σ , Hiess et al., 2012). All analyses, except those from samples 2116682 and 2131354, are -0.11 to 0.37% discordant. Analyses from sample 2116682 and 2131354 are up to 3.0% discordant (Fig. 6).

Errors on the weighted mean dates are quoted at the 95% confidence level and are the internal errors based on analytical uncertainties only, including counting statistics, subtraction of tracer solution, and blank

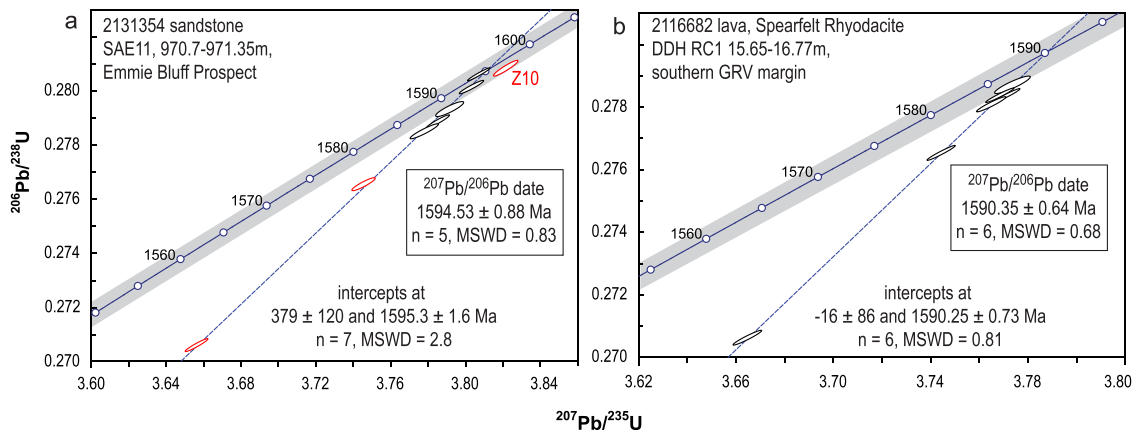


Fig. 6. Wetherill concordia plots of CA-TIMS analyses for the two samples with significant discordance, with intercept and weighted average ($^{207}\text{Pb}/^{206}\text{Pb}$) dates provided for comparison. Red ellipses represent analyses excluded from the $^{207}\text{Pb}/^{206}\text{Pb}$ weighted mean age calculation for sample 2131354. Two older analyses for sample 2131354 lie beyond the range of the plot.

and initial common Pb subtraction. Including the U decay constant uncertainties propagated in quadrature increases the errors, as reported in Table D2 of the supplementary dataset. Results are presented in Figs. 7 and 8.

Results

Lower Gawler range volcanics, Olympic Dam and surrounds

2131354 (SAE 11) is a sandstone with clastic components derived from two main sources: a silicic volcanic terrain and a granitic source. Zircon is subequant to elongate with strong oscillatory zoning and the grains have obvious metamict zones. The amount of discordance is substantially higher than most other samples in this study. Seven of ten zircons with varying degrees of Pb loss define a discordia with a lower intercept at c. 379 Ma and upper intercept at 1595.3 ± 1.6 Ma (Fig. 6a). The five most concordant of these analyses have a weighted mean $^{207}\text{Pb}/^{206}\text{Pb}$ date of 1594.5 ± 0.9 Ma (MSWD = 0.8, probability of fit = 0.51), in good agreement with the upper concordia intercept age. The two most discordant analyses on the discordia are interpreted to represent grains that experienced a considerable amount of ancient Pb loss (at c. 379 Ma). As a result, their younger $^{207}\text{Pb}/^{206}\text{Pb}$ ages are considered to have no geological significance. Three older dates of 1856.5 ± 1.3, 1812.4 ± 1.2 and 1599.5 ± 1.3 Ma are interpreted to represent grains with inherited components (cores), or detrital grains from an older source. The 1856.5 ± 1.3 Ma date reflects the age of the Palaeoproterozoic Donington Suite, which is a known basement component of the Olympic Dam region (Jagodzinski, 2005) (Fig. S3 of the supplementary text). The 1812.4 ± 1.2 Ma date could be a mixing age produced by a GRV volcanic zircon enclosing a Donington Suite core.

Zircon from dacite porphyry 2131365 (RED 2) is subequant to elongate with weak to moderate oscillatory zoning. Six $^{207}\text{Pb}/^{206}\text{Pb}$ dates yield a weighted mean of 1592.8 ± 0.7 Ma (MSWD = 1.7, probability of fit = 0.14).

Zircon from sericitised dyke 2000-366166 (RU45-4425, Olympic Dam deposit) is subequant with moderate to strong oscillatory zoning. Six $^{207}\text{Pb}/^{206}\text{Pb}$ dates yield a weighted mean of 1592.2 ± 0.7 Ma (MSWD = 0.7, probability of fit = 0.65). Another date of 1594.6 ± 1.2 Ma is from an older grain, possibly of antecrystic origin, or incorporated from the country rock as the dyke intruded older GRV and Hiltaba Suite of this age (Table 1). Another date of 1590.1 ± 1.2 Ma is interpreted as being from a grain that experienced ancient Pb loss.

Lower Gawler range volcanics, north-western volcanic centres

Zircon from ignimbrite 2016125 (Ealbara Rhyolite) is inclusion-rich and elongate with weak oscillatory zoning and central domains that are typically CL brighter than outer domains. Six $^{207}\text{Pb}/^{206}\text{Pb}$ dates yield a weighted mean of 1590.4 ± 0.6 Ma (MSWD = 0.3, probability of fit = 0.91).

Zircon from rhyolitic ignimbrite 2746487 (Chitanilga Volcanic Complex) is elongate with strong oscillatory zoning. Seven $^{207}\text{Pb}/^{206}\text{Pb}$ dates yield a weighted mean of 1589.2 ± 0.3 Ma (MSWD = 1.8, probability of fit = 0.10). Another date of 1588.5 ± 0.4 Ma is interpreted as being from a grain that experienced ancient Pb loss.

Zircon from dacite lava 2721839 (Mangaroonah Dacite, Glyde Hill Volcanic Complex) is small and equant with oscillatory and sector zoning. Five $^{207}\text{Pb}/^{206}\text{Pb}$ dates yield a weighted mean of 1589.2 ± 0.5 Ma (MSWD = 1.5, probability of fit = 0.19).

Lower Gawler range volcanics, southern margin of the Gawler ranges

Zircon from dacite porphyry 2017742 (Angle Dam Dacite) is inclusion rich and subhedral to elongate with moderate oscillatory zoning and central domains that are typically CL brighter than outer domains. Six $^{207}\text{Pb}/^{206}\text{Pb}$ dates yield a weighted mean of 1593.6 ± 0.2 Ma (MSWD = 0.7, probability of fit = 0.64).

Zircon from lava 2116682 (Spearfelt Rhyodacite, RC 1) is inclusion rich and elongate with strong oscillatory zoning. Discordance is substantially higher than any sample in this study except for 2,131,354, and six zircons with varying degrees of Pb loss define a discordia with a zero-age lower intercept, and upper intercept at 1590.3 ± 0.7 Ma (Fig. 6b). The six grains yield equivalent $^{207}\text{Pb}/^{206}\text{Pb}$ dates with a weighted mean of 1590.4 ± 0.7 Ma (MSWD = 0.7, probability of fit = 0.64), in excellent agreement with the upper concordia intercept age.

Zircon from rhyolite porphyry 2116683 (Map unit M15, RC1) is subequant to elongate with moderate oscillatory zoning. Six of the eight $^{207}\text{Pb}/^{206}\text{Pb}$ dates yield a weighted mean of 1590.1 ± 0.6 Ma (MSWD = 0.7, probability of fit = 0.6). Another date of 1593.0 ± 1.2 Ma is interpreted as being from an inherited grain, possibly an antecryst, and another of 1588.1 ± 1.3 Ma is interpreted as being from a grain that experienced ancient Pb loss.

Zircon from 2018616 (Bittali Rhyolite) is subequant to elongate with stronger oscillatory zoning than zircon in the other samples. Six $^{207}\text{Pb}/^{206}\text{Pb}$ dates yield a weighted mean of 1588.5 ± 0.7 Ma (MSWD = 0.3, probability of fit = 0.94).

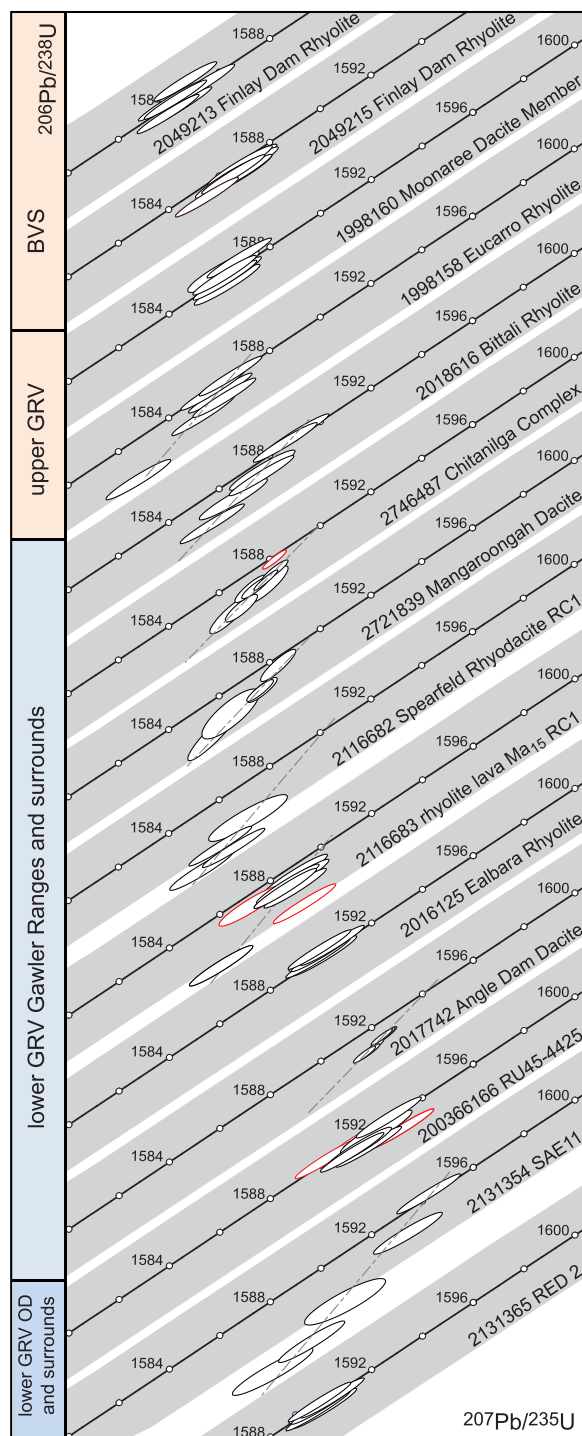


Fig. 7. Wetherill concordia plots of CA-TIMS analyses for the zircons in Fig. 5. The grey bands behind the concordia lines represent the 2σ decay constant uncertainty of concordia. Error ellipses are 2σ . Red ellipses represent analyses excluded from age interpretations. 2131354 (SAE 11) and 2116682 (Spearfeld Rhyodacite) have analyses that lie beyond the range of the plots (see Fig. 6).

Upper Gawler range volcanics

Zircon from rhyolite lava 1998158 (Eucarro Rhyolite) is inclusion-rich and elongate with weak oscillatory zoning. Six $^{207}\text{Pb}/^{206}\text{Pb}$ dates yield a weighted mean of 1586.7 ± 0.6 Ma (MSWD = 1.1, probability of fit = 0.38).

Zircon from dacite lava 1998160 (Moonaree Dacite Member) is similar to 1,998,158. Six $^{207}\text{Pb}/^{206}\text{Pb}$ dates yield a weighted mean of

1586.4 ± 0.7 Ma (MSWD = 0.6, probability of fit = 0.73).

Benagerie volcanic suite

Zircon from 2049215 (CU 1) is subequant to elongate with weak to moderate oscillatory zoning. Eight $^{207}\text{Pb}/^{206}\text{Pb}$ dates yield a weighted mean of 1587.3 ± 0.5 Ma (MSWD = 0.6, probability of fit = 0.80).

Zircon from rhyolite porphyry 2049213 (BRD013) is subequant to elongate with no zoning to weak oscillatory zoning. Six $^{207}\text{Pb}/^{206}\text{Pb}$ dates yield a weighted mean of 1586.4 ± 0.8 Ma (MSWD = 1.6, probability of fit = 0.16).

Discussion

Duration of volcanism and Hiltaba Suite magmatism

Due to its economic importance, the c. 1595 – 1575 Ma magmatic event has been dated more than any other time slice of South Australia's geological history (Tiddy & Giles, 2020 and references therein). Prior to recent high-precision CA-TIMS dating, the magmatic crystallisation age of over 200 samples of granite and volcanic rocks were determined using a variety of dating techniques, including multi-zircon/apatite/titanite ID-TIMS, SHRIMP, LA-ICPMS, Ar-Ar and Kober Pb evaporation (Table 1 and Supplementary Data Table D1) (Fig. 9). On average, the uncertainty in these analytical methods is 0.76% at the 95% confidence level, which corresponds to approximately 12 million years. The large and overlapping errors on the dates meant it was impossible to accurately determine the duration of volcanism and magmatism or establish temporal internal stratigraphic correlations for the Gawler LIP. However, some broad spatial trends could be discerned, with the data suggesting that the oldest volcanic and granitic rocks are in the subsurface at Olympic Dam and surrounding prospects. In particular, the Roxby Downs Granite of the Hiltaba Suite consistently produced dates of c. 1593 Ma (Jagodzinski, 2014) compared with dates mainly ranging between c. 1580 – 1590 Ma in other parts of the Gawler Craton. Tiddy & Giles (2020) noted a northeast to southwest progression from older to younger ages in the Hiltaba Suite, which is borne out when the data are plotted (Fig. 10). They postulate a north-south trending arc of older plutons ranging from Olympic Dam down into the Yorke Peninsula. However, when the data are contoured the pattern of younging propagates radially outward from the Olympic Dam area, especially when the Curnamona Province and Mount Painter Inlier are taken into consideration (Fig. 11a), in a temporal pattern suggestive of an upwelling mantle plume head rising and flattening out beneath the thick crust. Whereas most of the magmatism occurs between c 1595 and 1575 Ma, about 15% of the dates for granites are younger, between c. 1575 and 1530 Ma (Fig. 9). The younger granites are mainly in the Mt Painter and Mt Babbage Inliers, Curnamona Province, Yorke Peninsula, Peake and Denison Ranges and Fowler Domain, all located on the margins of the Gawler LIP and associated with contemporary metamorphism and deformation. Whether these younger dates record a separate event or are progressive from c. 1595 to 1575 Ma magmatism is not fully resolved, but it is likely they are related to slower cooling rates at deeper crustal levels, with crustal reworking partitioned into the less competent regions around the margins of a strong central upper crustal core where the GRV and Hiltaba Suite are preserved.

By careful control of laboratory conditions, particularly by reducing environmental Pb contamination and reducing discordance through chemical abrasion of the outer rims, the CA-TIMS method reduces analytical uncertainties to <0.05%, resolving ages to within one million years (e.g. Mattinson 2005, Metcalfe et al. 2015, Schaltegger et al. 2015). CA-TIMS dating has been used in recent studies to delineate the relative timing of magmatism, tectonic, sedimentary and mineralisation processes in the Fe oxide-Cu-Au-U deposits at Olympic Dam and Acropolis (Cherry et al., 2018; Courtney-Davies et al., 2019, 2020; McPhie et al., 2020), demonstrating the impact that high-precision

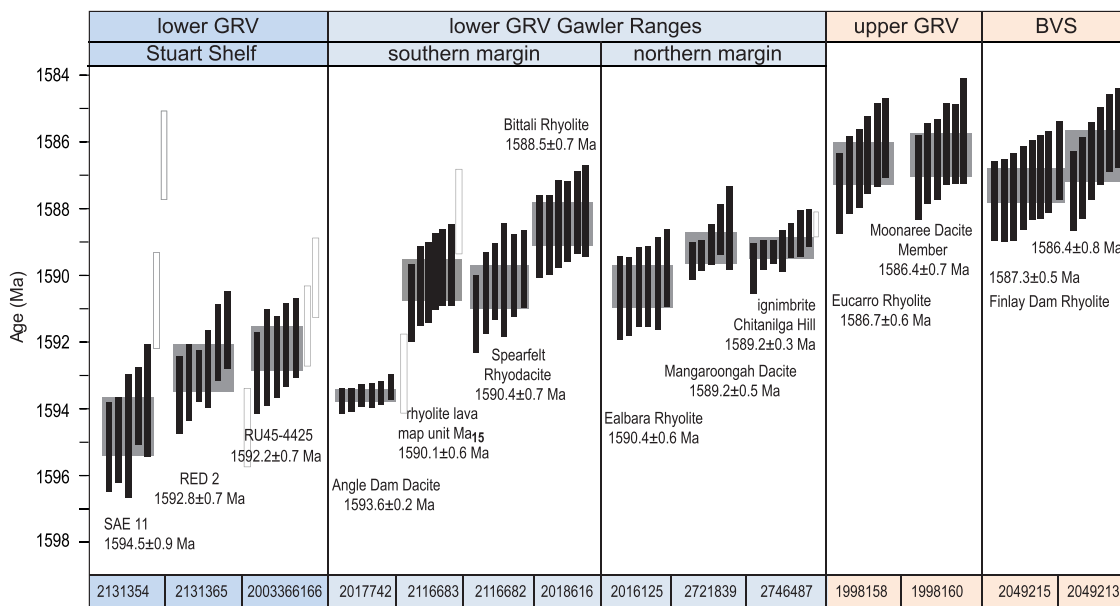


Fig. 8. Ranked box plot of $^{207}\text{Pb}/^{206}\text{Pb}$ dates from zircon CA-TIMS analyses. Black bars represent the 2σ errors on each analysis and white bars are excluded analyses. Grey boxes behind the error bars represent the weighted mean age for each sample and their 95% confidence error.

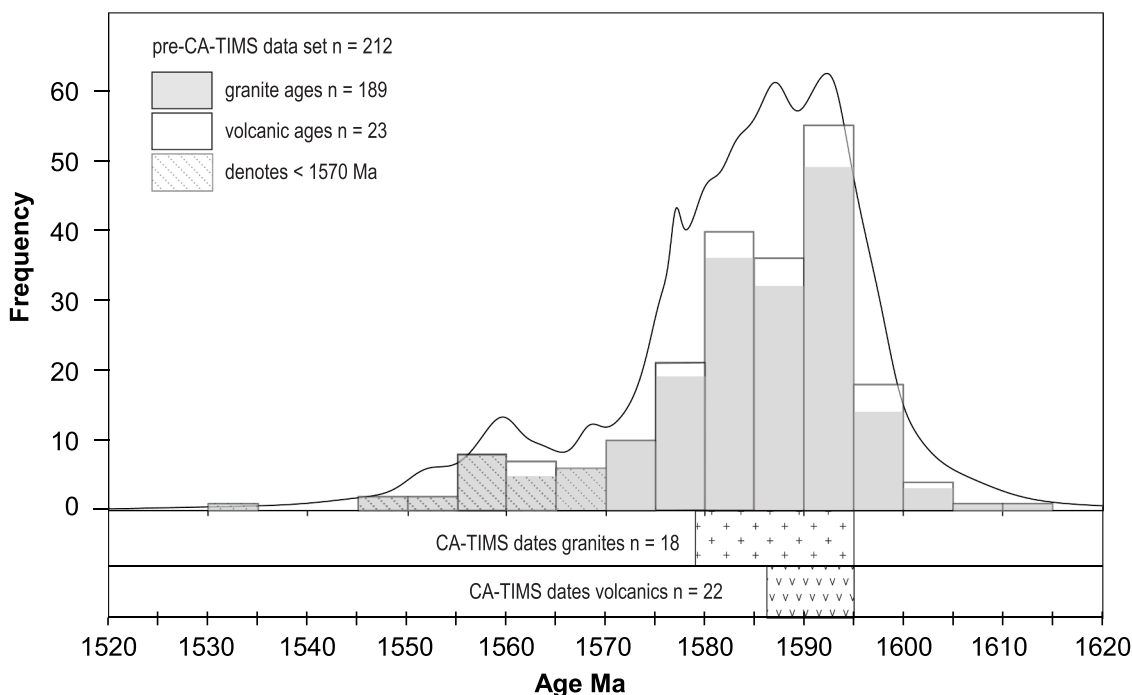


Fig. 9. The range of pre-CA-TIMS dates for volcanics and granites of the Gawler LIP, plotted as a probability density diagram (PDD) and histogram. The range of CA-TIMS dates for granite and volcanic rocks are plotted below the PDD for comparison.

dating can have on improving metallogenic modelling. This study expands the application of high precision dating to understand these processes on a regional scale. High-precision dates for the Hiltaba Suite (Jagodzinski et al., 2021; Reid et al., 2021, Supplementary Table D1) and GRV-BVS (Cherry et al., 2018; Courtney-Davies et al., 2019, 2020; McPhie et al., 2020 and this study, Tables 1, 2) reproduce the same radially-younging pattern with the Olympic Dam area as the locus, validating the spatial trends observed in the larger dataset of less precise ages (Fig. 10b).

Pre-CA-TIMS datasets produced ages for the GRV and BVS between c. 1575 and 1605 Ma which could imply a long-lived volcanic event of

about 30 million years (Table 1), although authors widely quoted a duration of about 2 million years for the volcanic succession based on the two most precise dates of 1591 ± 3 and 1592 ± 3 Ma for the lower and upper GRV, respectively (Fanning et al., 1988). The new CA-TIMS dates indicate that the entire volcanic province erupted over a geologically short time interval of less than 10 million years (c. 1594.5 – 1586.4 Ma) (Table 2). Following cessation of volcanism, intrusion of the Hiltaba Suite continued at least another 8 million years. To date, the youngest granite analysed by the CA-TIMS method is 1579.37 ± 1.57 Ma (Jagodzinski et al. 2021) indicating the entire thermal event lasted at least 16 million years and confirming previous estimates of c. 20 million

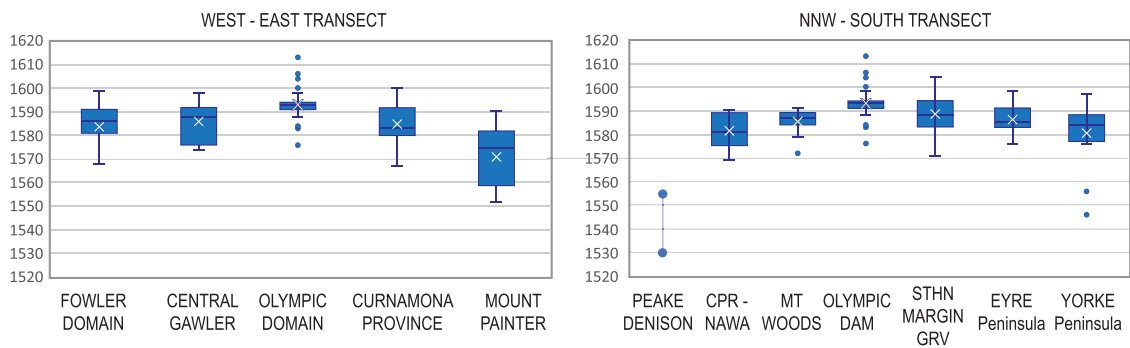


Fig. 10. Box and Whisker plots comparing the range of magmatic ages across domains of the Gawler Craton, Curnamona Province and Mt Painter Inlier. (CA-TIMS dates excluded). The white crosses represent the means of the populations, and the blue horizontal line represents the medians.

years for the duration of upper crustal magmatism (Table 1).

Temporal correlations of volcanic successions in the GRV-BVS

When establishing temporal correlations between volcanic units, pairwise comparisons were conducted to determine which samples are significantly different in age and which are statistically indistinguishable (supplementary text S1) (Fig. 12). From this, a chronostratigraphic framework is constructed for the Gawler LIP (Fig. 13).

There is significant age variance in the lower GRV, indicating the small, spatially isolated volcanic centres erupted as a series of discrete temporal events. As indicated by pre-CA-TIMS dating, earliest volcanism is recorded in the Olympic Dam region. The volcanoclastic sandstone from Emmie Bluff prospect (SAE11) contains the oldest zircons, the textural immaturity of the sandstone suggesting a proximal, possibly penecontemporaneous 1594.5 ± 0.9 Ma volcanic source. Volcanism continued in the region for the next c. 2.5 million years with emplacement of porphyritic rhyolites and dacites and aphanitic dykes at Olympic Dam, Acropolis and Red Dam. At the same time, 200 km to the south, the Angle Dam Dacite was emplaced in the Roopena Basin.

After a significant hiatus of 1–2 million years, the locus of volcanism shifted, commencing in the Gawler Ranges on both the northwestern and southeastern margins concurrently. On the northwestern margin, volcanism commenced at 1590.4 ± 0.6 Ma with eruption of the Ealbara Rhyolite and intercalated Konkaby Basalt north of Tarcoola. At the same time, a bimodal succession of coherent porphyritic rhyolite and dacite lavas and thick intervals of stacked basalt flows was deposited in a fluvio-lacustrine basin at Myall Creek (Simpson, 2017). Both these successions are the same age as the tuffaceous mudstones in the bedded clastic facies (BCF) at Olympic Dam (1590.1 ± 0.6 Ma, Cherry et al., 2018) and could have sourced the delicate bubble-wall shards and crystal fragments that settled from an ash cloud into the mudstones (McPhie et al., 2016). The explosive eruptions that formed the ignimbritic Ealbara Rhyolite are the better candidate. Although the sedimentary basins at Olympic Dam and Myall Creek are contemporary, the Roopena Basin, which is located about 30 km to the south of Myall Creek, is at least 3 million years older. This indicates that the few preserved examples of sedimentary basins in the lower GRV, all located in the eastern Gawler Craton (at Roopena, Myall Creek, Olympic Dam and Prominent Hill), are not relics of one large, connected basin.

About one million years later, the Chitanilga Volcanic Complex and Glyde Hill Volcanic Complex erupted synchronously in the northwest at 1589.19 ± 0.48 Ma, followed shortly after by the Bitali Rhyolite from multiple eruption points along the southern margin, including the Menninnie Dam volcanic centre, at 1588.7 ± 0.66 Ma.

Bimodal volcanism of the lower GRV lasted about 6 million years, from c. 1594.5 to 1588.5 Ma, following which another significant hiatus of 1–2 million years marks a distinctive change in the style of eruptive volcanism, with the onset of large-scale effusive eruptions forming the flood rhyolite province of the upper GRV (Fig. 13). The Eucarro Rhyolite

(1586.7 ± 0.6 Ma) and Moonaree Dacite Member of the Yardea Dacite (1586.4 ± 0.7 Ma), have crystallisation ages that are indistinguishable. With estimated volumes for the lavas ranging from 1000 to 4000 km³ each (Allen et al., 2003), the dates indicate that c. 3000–12,000 km³ of silicic magma erupted in under 1.5 million years, and probably as rapidly as a few hundred thousand years. The resultant high magma flux rates would have contributed to the extensive outflow of the upper GRV lavas. The stratigraphy and facies architecture of the BVS has not been established due to poor drill hole coverage of the unit, but the lavas have been correlated with upper GRV based on a shared geochemical and isotopic affinity (Wade et al. 2012), which is confirmed by the CA-TIMS dates. The slightly older date for the Finlay Dam Rhyolite in drill hole CU1 suggests high-volume volcanism might have commenced slightly earlier in the Curnamona Province.

Comparison with continental flood basalt provinces: a modern analogue

A defining feature of LIPs is that they represent large volume igneous events (> 0.1 Mkm³) of short duration (Bryan & Ernst, 2008; Bryan & Ferrari, 2013; Coffin & Eldholm, 1994). LIPs are estimated to have a maximum possible duration of c. 50 Myr, but many span less than 10–15 Myr. The longer-lived LIPs with age spans > 15 Myr are emplaced in shorter episodes of 1–5 Myr duration, rather than as a continuous long-lasting magmatic event (Bryan & Ernst, 2008). LIPs are most widely recognised as voluminous outpourings of low-viscosity basaltic lava, which occur on both continental and oceanic crust (Ernst, 2014 and references therein). However, silicic volcanism is recognised as a significant component of continental LIPs, which are commonly ascribed to the presence of a thermal anomaly such as a mantle plume head beneath continental lithosphere, with mantle-derived basaltic melts triggering large-scale melting in the overlying crust (Bryan & Ernst, 2008; Bryan et al., 2002).

With mafic volcanic rocks comprising less than 5% of the preserved volcanic succession, the Gawler LIP is recognised as a silicic end member of terrestrial LIPs, which are more typically dominated by mafic magmatism (Pankhurst et al., 2011b). The duration of volcanism in the Gawler LIP (c. 8 Myr) is comparable to that of Continental Flood Basalt Provinces (CFBPs) which, with a typical life span of 5–10 Myr, are the shortest-lived events in the LIP family (Bryan & Ernst, 2008; Courtillot & Renne, 2003; Jerram & Widdowson, 2005). The elliptical-shaped central province is analogous to the geometries of CFBPs. The total eruption volume of the silicic dominated Gawler LIP is small compared to its mafic counterparts. It is about half the size of the smallest CFBP (the Columbia River flood basalt province, c. 210,000 km³, Barry et al., 2013; Camp et al., 2003). One of the key geological features of LIPs is the pulsed nature of magmatism, where relatively large volumes of magma are erupted and emplaced in a short period of time (Bryan & Ernst, 2008; Bryan & Ferrari, 2013). Although this was widely considered to be the case for the upper GRV lavas (Agangi et al., 2012; Allen et al., 2008; Pankhurst et al., 2011b), it was not fully apparent in the previous age

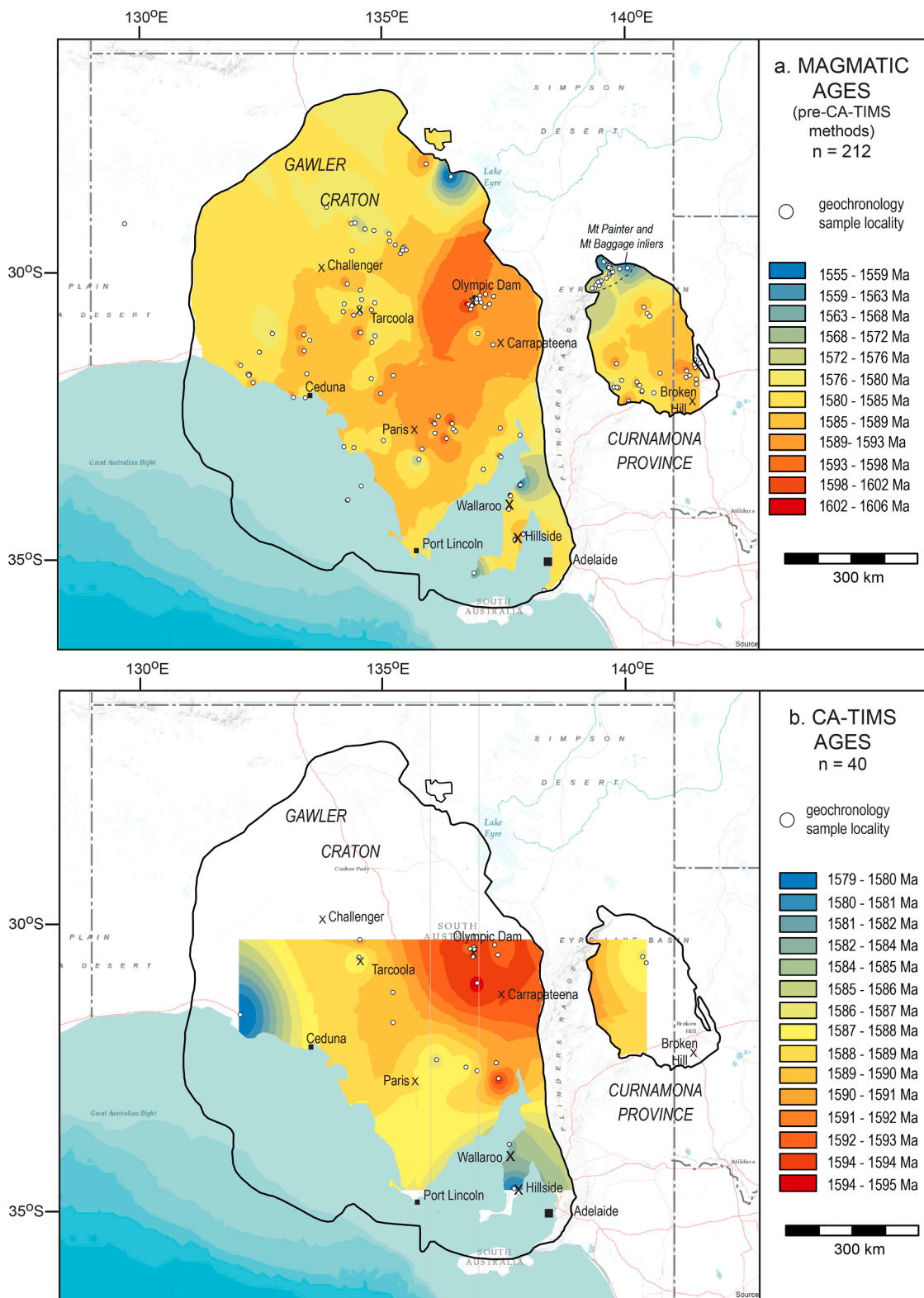


Fig. 11. Contour maps of magmatic ages for the Gawler Lip, showing the progression of magmatism. Magmatism initiated in the Olympic Dam region, then progressed radially outward, in a temporal pattern suggestive of a rising and flattening plume head. (a) Pre-CA-TIMS data. (b) High-precision CA-TIMS dates.

data but is now confirmed, with volumes of c. 3000–12,000 km³ erupted in c. 260 000 years.

CFBPs and their silicic components provide a modern analogue for the GRV LIP. The chrono-stratigraphic framework now constructed for the GRV-BVS (Fig. 13) allows the anatomy of these provinces to be compared. Jerram & Widdowson (2005) recognised that Phanerozoic

CFBPs are composed of a series of discrete volcanic successions which can be broadly grouped into three identifiable phases; (i) an initiation phase; (ii) a main phase, ‘pulse’ or acme; and (iii) a waning phase. Periods of quiescence occur during these phases, as evidenced by the presence of weathering horizons, sedimentation and erosion surfaces, representing periods of 10 – 10,000 years. CFBPs initially begin with

total volume of the Columbia River Flood Basalt Province erupted between 16.6 and 15.3 Ma (Barry et al., 2013; Camp et al., 2003). The waning phase returns to a significant decrease in eruption volumes from more widely distributed volcanic centres, longer hiatuses between successive eruptive episodes, commonly with increasing silica content and highly explosive eruptive products.

The first two phases of the CFBP model can be recognised within the Gawler LIP, with the lower GRV representing the initial phase involving a relatively prolonged period of volcanism (c. 6 Myr) as low-volume bimodal eruptions from discrete, isolated volcanic centres, and the upper GRV representing the short-lived (c. 260 000 years) main phase during which the thick, regionally extensive rhyolite and dacite lavas erupted. As with the larger mafic volcanic fields, relatively short periods of quiescence between eruptions are marked by thin, regionally extensive horizons of pyroclastic, volcanoclastic and volcanogenic sedimentary rocks (e.g. Mount Friday Formation, Mount Double Ignimbrite, Nonning Sandstone, Yartoo volcanoclastics, Werner et al., 2017). A longer hiatus of c. 1–2 Myr marks a change in the locus of volcanism in the lower GRV from east (Olympic Dam region and Roopena Basin) to west (northwestern volcanic centres and southwest margin of the Gawler Ranges). A significant hiatus of similar duration separates the initial and main stages of eruption represented by the lower and upper GRV, respectively. The third, waning stage of Jerram & Widdowson (2005), is not preserved in the geological record and might not have existed. However, magmatism was ongoing after the volcanic component ceased to erupt, with emplacement of shallow-level intrusions of the Hiltaba Suite.

Conclusions

The ability to resolve crystallisation ages within volcanic sequences that accumulated in a very short time span is critical to understanding the temporal history of these short-lived provinces, and delineating eruptive patterns requires precise geochronological control (≤ 1 Myr). High-precision CA-TIMS zircon dating reveals how the Gawler LIP is constructed spatially and temporally, determining the duration of volcanism and eruptive history of the province. This study establishes a chronostratigraphic framework for the Mesoproterozoic Gawler LIP, in which extreme quantities of silicic magma erupted in a short time frame culminating in the development of a flood rhyolite province, the volume and areal extent of which are analogous to the Phanerozoic continental flood basalt provinces.

The new dates support previous estimates that upper crustal magmatism lasted approximately 20 Myr with the lower GRV spanning c. 6 Myr, commencing in the Olympic Dam region. Here, volcanism and contemporary granitoid emplacement extended between c. 1595–1592 Ma. Where both have been dated at Olympic Dam and Acropolis, the Hiltaba Suite is interpreted to have intruded the GRV, although their crystallisation ages are statistically indistinguishable. After a significant hiatus of 1–2 Myr the locus of volcanism shifted west, where eruption of the lower GRV in the central Gawler Craton continued for another c. 2 Myr between c. 1590.5–1588.5 Ma. The small, syn-volcanic fluvio-lacustrine basins of the lower GRV preserved in the eastern Gawler Craton are not all contemporary in age, and therefore not relics of one large, connected basin.

Another significant hiatus of 1–2 Myr marks the boundary between the lower and upper GRV with their two distinctive eruption styles. Magmatism then culminated in large volume eruptions producing an extensive flood rhyolite province over a short period of c. 260 000 years. The entire volcanic province erupted over a time interval of c. 8 Myr. Following cessation of volcanism, intrusion of the Hiltaba Suite continued at least another 8 million years.

The anatomy of the Gawler LIP is comparable to that of CFBPs, which record similar eruptive histories, initially beginning with a lengthy period of geographically scattered low-volume eruptions then switching to a main eruptive pulse of comparatively short duration, typically

characterised by large volume tabular flows and extensive flow fields. The final stage in the life span of a CFBP, marked by a return to significantly smaller erupted volumes and longer hiatuses between successive eruptive episodes, is not preserved in the Gawler LIP.

Recognising the salient similarities to continental mafic LIPs helps to understand the underlying geological processes involved in generating the silicic Gawler LIP. Continental LIPs are commonly associated with spatially constrained, transient thermal melting anomalies in the upper mantle (Ernst, 2014 and references therein; Ernst & Buchan, 2003). Whether these are related to mantle plumes or other mechanisms such as lithospheric underplating, the temporal, spatial, and volcanological characteristics can be used to constrain geochemical or geophysical models, to help understand the underlying tectonic processes. The revised stratigraphy and regional correlation between units of the GRV provide an opportunity to study the geochemical and isotopic evolution of the Gawler LIP, with respect to mantle evolution and crustal melting behaviour and mantle source input, which is explored in a companion paper in this volume (Wade et al., 2022).

Declaration of Competing Interest

The authors declare that they have no known competing financial interests or personal relationships that could have appeared to influence the work reported in this paper.

Data availability

Data are included in the supplementary material

Acknowledgments

Dr Simon Bodorkis of Geoscience Australia assisted with protocols for error reporting and error propagation (supplementary paper S1). Petrographic descriptions in supplementary paper S2 are by Dr Doug Mason of Mason Geoscience Pty Ltd. Dr Mario Werner (GSSA) provided the description of drill hole RED 2 in supplementary paper S2. Stephen Hore (GSSA) assisted with collection of some GRV samples. Constructive reviews on an earlier version of this manuscript by Dr Scott Bryan and an anonymous reviewer significantly improved the paper. Reviews by Dr Ashley Gumsley and an anonymous reviewer also improved the quality of this version.

Supplementary materials

Supplementary material associated with this article can be found, in the online version, at [doi:10.1016/j.ringeo.2022.100020](https://doi.org/10.1016/j.ringeo.2022.100020).

References

- Agangi, A., Kamenetsky, V. S., & McPhie, J. (2012). Evolution and emplacement of high fluorine rhyolites in the Mesoproterozoic Gawler silicic large igneous province, South Australia. *Precambrian Research*, 208–211, 124–144. <https://doi.org/10.1016/j.precamres.2012.03.011>
- Allen, S. R., McPhie, J., Ferris, G., & Cadd, A. G. (2008). Evolution and architecture of a large felsic igneous province in western Laurentia: The 1.6 Ga Gawler Range Volcanics, South Australia. *Journal of Volcanology and Geothermal Research*, 172, 132–147. <https://doi.org/10.1016/j.jvolgeores.2005.09.027>
- Allen, S. R., & McPhie, J. (2002). The Eucarro Rhyolite, Gawler Range Volcanics, South Australia; a >675 km³ compositionally zoned lava of Mesoproterozoic age. *Geological Society of America Bulletin*, 114, 1592–1609. [https://doi.org/10.1130/0016-7606\(2002\)114<1592:TERGRV>2.0.CO;2](https://doi.org/10.1130/0016-7606(2002)114<1592:TERGRV>2.0.CO;2)
- Allen, S. R., Simpson, C. J., McPhie, J., & Daly, S. J. (2003). Stratigraphy, distribution and geochemistry of widespread felsic volcanic units in the Mesoproterozoic Gawler Range Volcanics, South Australia. *Australian Journal of Earth Sciences*, 50, 97–112. <https://doi.org/10.1046/j.1440-0952.2003.00980.x>
- Barry, T. L., Kelley, S. P., Reidel, S. P., Camp, V. E., Self, S., Jarboe, N. A., et al. (2013). Eruption chronology of the Columbia River Basalt Group. In S. P. Reidel, V. E. Camp, M. E. Ross, J. A. Wolff, B. S. Martin, T. L. Tolani, et al. (Eds.), *The Columbia river flood Basalt Province* (pp. 45–66). Geological Society of America Special Paper 497. [https://doi.org/10.1130/2013.2497\(02\)](https://doi.org/10.1130/2013.2497(02))

- Belperio, A., Flint, R. B., & Freeman, H. (2007). Prominent Hill: A hematite dominated, iron oxide copper–gold system. *Economic Geology*, 102, 1499–1510. <https://doi.org/10.2113/gsecongeo.102.8.1499>
- Blissett, A. H., Creaser, R. A., Daly, S., Flint, D. J., & Parker, A. J. (1993). Gawler range volcanics. In J. F. Drexel, W. V. Preiss, & A. J. Parker (Eds.), *The geology of South Australia* (pp. 107–131). Geological Survey of South Australia. vol 1. the precambrian, Bulletin 54, Adelaide [https://sarigbasis.pir.sa.gov.au/WebtopEw/ws/samref/sarig1/image/DDD/BULL054\(V1\).pdf](https://sarigbasis.pir.sa.gov.au/WebtopEw/ws/samref/sarig1/image/DDD/BULL054(V1).pdf).
- Blissett, A. H. (1975). Rock units in the Gawler Range Volcanics, South Australia. Quarterly Geological Notes 55. *Geological Survey of South Australia*, 2–14. <https://sarigbasis.pir.sa.gov.au/WebtopEw/ws/samref/sarig1/image/DDD/QGN055.pdf>.
- Branch, C. D. (1978). Evolution of the middle proterozoic Chandabook Caldera, Gawler Range acid volcano-plutonic province, South Australia. *Journal of the Geological Society of Australia*, 25, 199–216. <https://doi.org/10.1080/00167617808729028>
- Bryan, S. E., & Ernst, R. E. (2008). Revised definition of large igneous provinces (LIPs). *Earth-Science Reviews*, 86, 175–202. <https://doi.org/10.1016/j.earscirev.2007.08.008>
- Bryan, S. E., & Ferrari, L. (2013). Large igneous provinces and silicic large igneous provinces: Progress in our understanding over the last 25 years. *Geological Society of America Bulletin*, 125, 1053–1078. <https://doi.org/10.1130/B30820.1>
- Bryan, S. E., Riley, T. R., Jerram, D. A., Leat, P. T., & Stephens, C. J. (2002). Silicic volcanism: An under-valued component of large igneous provinces and volcanic rifted margins. In M. A. Menzies, S. L. Klemperer, C. J. Ebinger, & J. Baker (Eds.), *Magmatic rifted margins* (pp. 99–118). Geological Society of America. Special Paper 362 <http://www.mantleplumes.org/WebDocuments/Bryanetal2002.pdf>.
- Bull, S., Meffre, S., Allen, M., Freeman, H., Tomkinson, M., & Williams, P. (2015). Volcanosedimentary and chronostratigraphic architecture of the host rock succession at prominent Hill, South Australia. seg 2015: World-class ore deposits: Discovery to recovery, Hobart, Tasmania, Society of Economic Geologists, pp. abstract. http://www.segweb.org/SEG/Events/Conference_Archives/2015/Conference_Proceedings/files/pdf/Oral-Presentations/Abstracts/Bull.pdf.
- Camp, V. E., Ross, M. E., & Hanson, W. E. (2003). Genesis of flood basalts and Basin and Range volcanic rocks from Steens Mountain to the Malheur River Gorge, Oregon. *Geological Society of America Bulletin*, 115, 105–128. [https://doi.org/10.1130/0016-7606\(2003\)115<0105:GOFBAB>2.0.CO;2](https://doi.org/10.1130/0016-7606(2003)115<0105:GOFBAB>2.0.CO;2)
- Chapman, N. D., Ferguson, M., Meffre, S. J., Stepanov, A., Maas, R., & Ehrig, K. J. (2019). Pb-isotopic constraints on the source of A-type Suites: Insights from the Hiltaba Suite - Gawler Range Volcanics Magmatic Event, Gawler Craton, South Australia. *Lithos*, 346–347, Article 105156. <https://doi.org/10.1016/j.lithos.2019.105156>
- Cherry, A. R., Ehrig, K., Kamenetsky, V. S., McPhie, J., Crowley, J. L., & Kamenetsky, M. B. (2018). Precise geochronological constraints on the origin, setting and incorporation of ca. 1.59 Ga surficial facies into the Olympic Dam Breccia Complex, South Australia. *Precambrian Research*, 315, 162–178. <https://doi.org/10.1016/j.precamres.2018.07.012>
- Coffin, M. F., & Eldholm, O. (1994). Large igneous provinces: Crustal structure, dimensions, and external consequences. *Reviews of Geophysics*, 32, 1–36. <https://doi.org/10.1029/93RG02508>
- Conor, C. C. H., & Preiss, W. V. (2008). Understanding the 1720–1640 Ma Palaeoproterozoic Willyama Supergroup, Curramona Province, southeastern Australia: Implications for tectonics, basin evolution and ore genesis. *Precambrian Research*, 166, 297–317. <https://doi.org/10.1016/j.precamres.2007.08.020>
- Courtillot, V. E., & Renne, P. R. (2003). On the ages of flood basalt events. *Comptes Rendus Geoscience*, 335, 113–140. [https://doi.org/10.1016/S1631-0713\(03\)00006-3](https://doi.org/10.1016/S1631-0713(03)00006-3)
- Courtney-Davies, L., Ciobanu, C., Tapster, S., Cook, N., Ehrig, K., Crowley, J., & Condon, D. (2020). Opening the magmatic-hydrothermal window: High-precision U-Pb Geochronology of the Mesoproterozoic Olympic Dam Cu-U-Au-Ag deposit, South Australia. *Economic Geology*, 115(8), 1855–1870. <https://doi.org/10.5382/econgeo.4772>
- Courtney-Davies, L., Tapster, S. R., Ciobanu, C. L., Cook, N. J., Verdugo-Ihl, M. R., Ehrig, K., & Wade, B. P. (2019). A multi-technique evaluation of hydrothermal hematite U-Pb isotope systematics: Implications for ore deposit geochronology. *Chemical Geology*, 513, 54–72. <https://doi.org/10.1017/S1431927621009648>
- Creaser, R. A., & Cooper, J. A. (1993). U-Pb geochronology of middle proterozoic felsic magmatism surrounding the olympic dam Cu-U-Au-Ag and Moonta Cu-Au-Ag deposits, South Australia. *Economic Geology*, 88, 186–197. <https://doi.org/10.2113/gsecongeo.88.1.186>
- Creaser, R. A., & White, A. J. R. (1991). Yardea Dacite; large-volume, high-temperature felsic volcanism from the middle Proterozoic of South Australia. *Geology*, 19, 48–51. [https://doi.org/10.1130/0091-7613\(1991\)019<0048:YDLVHT>2.3.CO;2](https://doi.org/10.1130/0091-7613(1991)019<0048:YDLVHT>2.3.CO;2)
- Creaser, R. A. (1995). Neodymium isotopic constraints for the origin of Mesoproterozoic felsic magmatism, Gawler Craton, South Australia. *Canadian Journal of Earth Sciences*, 32, 460–471. <https://doi.org/10.1139/e95-039>
- Curtis, S. O., Wade, C. E., & Reid, A. J. (2018). Sedimentary basin formation associated with a silicic large igneous province: Stratigraphy and provenance of the Mesoproterozoic Roopena Basin, Gawler Range Volcanics. *Australian Journal of Earth Sciences*, 65, 447–463. <https://doi.org/10.1080/08120099.2018.1460398>
- Daly, S. J. (1985). Taroona map sheet. South Australia, geological survey. *Geological Atlas*, 1, 250 000 Series, sheet SH53-20 <https://sarigbasis.pir.sa.gov.au/WebtopEw/ws/plans/sarig1/image/DDD/200471-065>.
- Ernst, R. E., Bleeker, W., Söderlund, U., & Kerr, A. C. (2013). Large Igneous Provinces and supercontinents: Toward completing the plate tectonic revolution. *Lithos*, 174, 1–14. <https://doi.org/10.1016/j.lithos.2013.02.017>
- Ernst, R. E., & Buchan, K. L. (2003). Recognizing mantle plumes in the geological record. *Annual Review of Earth and Planetary Sciences*, 31, 469–523. <https://doi.org/10.1146/annurev.earth.31.100901.145500>
- Ernst, R. E., & Jowitt, S. M. (2013). Large Igneous Provinces (LIPs) and Metallogeny. In M. Colpron, T. Bissig, B. G. Rusk, & J. F. H. Thompson (Eds.), *Tectonics, metallogeny, and discovery: The North American Cordillera and similar accretionary settings* (pp. 17–51). Society of Economic Geologists. <https://doi.org/10.5382/SP.17.02>
- Ernst, R. E. (2014). *Large igneous provinces*, 653. Cambridge, UK: Cambridge University Press. <https://doi.org/10.1017/CBO9781139025300>
- Fanning, C. M., Flint, R. B., Parker, A. J., Ludwig, K. R., & Blissett, A. H. (1988). Refined Proterozoic evolution of the Gawler Craton, South Australia, through U-Pb zircon geochronology. *Precambrian Research*, 40–41, 363–386. [https://doi.org/10.1016/0301-9268\(88\)90076-9](https://doi.org/10.1016/0301-9268(88)90076-9)
- Fanning, C.M., Reid A.J. and Teale G.S. 2007. A geochronological framework for the Gawler Craton, South Australia, geological survey, bulletin 55. Department of Primary Industries and Resources South Australia, Adelaide. <https://sarigbasis.pir.sa.gov.au/WebtopEw/ws/samref/sarig1/wcir/Record>.
- Flint, R.B., Blissett, A.H., Conor, C.H.H., Cowley, W.M., Cross, K.C., Creaser, R.A. et al. (1993). Mesoproterozoic. in drexel JF, preiss wv and parker aj eds, the geology of south australia, volume 1, the Precambrian, Adelaide, bulletin - geological survey of South Australia: Geological Survey of South Australia, Bulletin 54, 106–169. ISBN 0730841464. [https://sarigbasis.pir.sa.gov.au/WebtopEw/ws/samref/sarig1/image/DDD/BULL054\(V1\).pdf](https://sarigbasis.pir.sa.gov.au/WebtopEw/ws/samref/sarig1/image/DDD/BULL054(V1).pdf).
- Forbes, C. J., Betts, P. G., Weinberg, R., & Buick, I. S. (2005). A structural metamorphic study of the Broken Hill Block, NSW, Australia. *Journal of Metamorphic Geology*, 23 (8), 745–770. <https://doi.org/10.1111/j.1525-1314.2005.00608.x>
- Garner, A., & McPhie, J. (1999). Partially melted lithic megablocks in the Yardea Dacite, Gawler Range Volcanics, Australia: implications for eruption and emplacement mechanisms. *Bulletin of Volcanology*, 61, 396–410. <https://doi.org/10.1007/s004450050281>
- Giles, C. W., & Teale, G. (1979). The geochemistry of Proterozoic acid volcanics from the Frome Basin. *Quarterly Geological Notes - Geological Survey of South Australia*, 71, 13–18. <https://sarigbasis.pir.sa.gov.au/WebtopEw/ws/samref/sarig1/image/DDD/QGN071.pdf>.
- Giles, C. W. (1988). Petrogenesis of the proterozoic Gawler Range volcanics, South Australia. *Precambrian Research*, 40–41, 407–427. [https://doi.org/10.1016/0301-9268\(88\)90078-2](https://doi.org/10.1016/0301-9268(88)90078-2)
- Hiess, J., Condon, D. J., McLean, N., & Noble, S. R. (2012). ²³⁸U/²³⁵U systematics in terrestrial uranium-bearing minerals. *Science*, 335, 1610–1614. <https://doi.org/10.1126/science.1215507> (New York, N.Y.).
- Jaffey, A. H., Flynn, K. F., Glendenin, L. F., Bentley, W. C., & Essling, A. M. (1971). Precision measurements of half-lives and specific activities of ²³⁵U and ²³⁸U. *Physical Review*, C4, 1889–1906. <https://doi.org/10.1103/PhysRevC.4.1889>
- Jagodzinski E.A., Crowley J.L., Reid A.J., Wade C.E. and Bockmann M.J. 2021. High-precision ca-tims dating of the hiltaba suite, Gawler craton. report book 2021/00002. Department for Energy and Mining, South Australia, Adelaide. <https://sarigbasis.pir.sa.gov.au/WebtopEw/ws/samref/sarig1/image/DDD/RB202100002.pdf>.
- Jagodzinski, E.A., Szpunar, M., Meaney, K., & Fraser, G. (2020). SHRIMP U-Pb dating of the barossa complex, south australia: Exploring tectonic links between the Gawler craton and Curramona province. report book 2020/00017, South Australia, Adelaide: Department for Energy and Mining. <https://sarigbasis.pir.sa.gov.au/WebtopEw/ws/samref/sarig1/image/DDD/RB202000017.pdf>.
- Jagodzinski, E. A. (2005). Compilation of SHRIMP U-Pb geochronological data – Olympic Domain, Gawler Craton, South Australia, 2001–2003. *AGSO Record 2005/20*, 197. <https://doi.org/10.13140/RG.2.2.10591.12962>
- Jagodzinski, E.A. (2014). The age of magmatic and hydrothermal zircon at olympic dam. In geological society of Australia, Abstracts No. 110, p. 260 and poster Australian earth sciences convention 2014, Newcastle, Australia. [10.13140/RG.2.2.10601.62569](https://doi.org/10.13140/RG.2.2.10601.62569).
- Jerram, D. A., & Widdowson, M. (2005). The anatomy of continental flood basalt provinces: Geological constraints on the processes and products of flood volcanism. *Lithos*, 79, 385–405. <https://doi.org/10.1016/j.lithos.2004.09.009>
- Johnson, J. P., & Cross, K. C. (1995). U-Pb geochronological constraints on the genesis of the Olympic Dam Cu-U-Au-Ag deposit, South Australia. *Economic Geology*, 90, 1046–1063. <https://doi.org/10.2113/gsecongeo.90.5.1046>
- Lloyd, J. C., Blades, M., Counts, J. W., Collins, A. S., Amos, K. J., Wade, B. P., et al. (2020). Neoproterozoic geochronology and provenance of the Adelaide Superbasin. *Precambrian Research*, 350. <https://doi.org/10.1016/j.precamres.2020.105849>
- Ludwig, K. R. (2012). Isoplot 3.75 - a geochronological toolkit for Microsoft Excel. *Berkeley Geochronology Center Special Publication No. 5*. <https://www.bgc.org/isoplot>.
- Manley, C. R. (1992). Extended cooling and viscous flow of large, hot rhyolite lavas: Implications of numerical modelling results. *Journal of Volcanology and Geothermal Research*, 53, 27–46. [https://doi.org/10.1016/0377-0273\(92\)90072-L](https://doi.org/10.1016/0377-0273(92)90072-L)
- Mattinson, J. M. (2005). Zircon U–Pb chemical abrasion (“CA-TIMS”) method: Combined annealing and multi-step partial dissolution analysis for improved precision and accuracy of zircon ages. *Chemical Geology*, 220, 47–66. <https://doi.org/10.1016/j.chemgeo.2005.03.011>
- McAvaney, S.O., & Wade, C.E. (2015). Stratigraphy of the lower gawler range volcanics in the Roopena area, north-eastern eyre peninsula, report book 2015/00021, South Australia, Adelaide: Department of State Development. <https://sarigbasis.pir.sa.gov.au/WebtopEw/ws/samref/sarig1/image/DDD/RB201500021.pdf>.
- McPhie, J., DellaPasqua, F., Allen, S. R., & Lackie, M. A. (2008). Extreme effusive eruptions: Palaeoflow data on an extensive felsic lava in the Mesoproterozoic gawler range volcanics. *Journal of Volcanology and Geothermal Research*, 172, 148–161. <https://doi.org/10.1016/j.jvolgeores.2006.11.011>
- McPhie, J., Ehrig, K., Kamenetsky, M. B., Crowley, J. L., & Kamenetsky, V. S. (2020). Geology of the acropolis prospect, South Australia, constrained by high precision CA-TIMS ages. *Australian Journal of Earth Sciences*, 67(5), 699–716. <https://doi.org/10.1080/08120099.2020.1717617>

- McPhie, J., Orth, K., Kamenetsky, V., Kamenetsky, M., & Ehrig, K. (2016). Characteristics, origin and significance of Mesoproterozoic bedded clastic facies at the Olympic Dam Cu–U–Au–Ag deposit, South Australia. *Precambrian Research*, 276, 85–100. <https://doi.org/10.1016/j.precamres.2016.01.029>
- Metcalfe, I., Crowley, J. L., Nicoll, R., & Schmitz, M. (2015). High-precision U–Pb CA–TIMS calibration of middle permian to lower triassic sequences, mass extinction and extreme climate-change in eastern Australian Gondwana. *Gondwana Research*, 28, 61–81. <https://doi.org/10.1016/j.gr.2014.09.002>
- Morrow, N., & McPhie, J. (2000). Mingled silicic lavas in the mesoproterozoic gawler range volcanics, South Australia. *J. Volcanol. Geotherm. Res.*, 96, 1–13. [https://doi.org/10.1016/S0377-0273\(99\)00143-2](https://doi.org/10.1016/S0377-0273(99)00143-2)
- Mortimer, G. E., Cooper, J. A., Paterson, H. L., Cross, K., Hudson, G. R. T., & Uppill, R. K. (1988). Zircon U–Pb dating in the vicinity of the olympic dam Cu–u–Au deposit, Roxby Downs, South Australia. *Economic Geology*, 83, 694–709. <https://doi.org/10.2113/gsecongeo.83.4.694>
- Myers, J. S., Shaw, R. D., & Tyler, I. M. (1996). Tectonic evolution of proterozoic Australia. *Tectonics*, 15, 1431–1446. <https://doi.org/10.1029/96TC02356>
- Page, R. W., Stevens, B. P. J., & Gibson, G. M. (2005). Geochronology of the sequence hosting the broken hill Pb–Zn–Ag orebody, Australia. *Econ. Geol.*, 100, 633–661. <https://doi.org/10.2113/gsecongeo.100.4.633>
- Pankhurst, M. J., Schaefer, B. F., Betts, P. G., Phillips, N., & Hand, M. (2011b). A Mesoproterozoic continental flood rhyolite province, the Gawler Ranges, Australia: The end member example of the large igneous Province clan. *Solid Earth*, 2, 25–33. <https://doi.org/10.5194/se-2-25-2011>
- Pankhurst, M. J., Schaefer, B. F., & Betts, P. G. (2011a). Geodynamics of rapid voluminous felsic magmatism through time. *Lithos*, 123, 92–101. <https://doi.org/10.1016/j.lithos.2010.11.014>
- Reid, (2019). The olympic Cu–Au Province, Gawler Craton: a review of the lithospheric architecture, geodynamic setting, alteration systems, cover successions and prospectivity. *Minerals*, 9, 371. <https://doi.org/10.3390/min9060371>
- Reid A.J, & Jagodzinski E.A. E (2012).ds.PACE geochronology: Results of collaborative geochronology projects 2011–12. Report book 2012/00012, South Australia, Adelaide: Department for Manufacturing, Innovation, Trade, Resources and Energy. <https://sarigbasis.pir.sa.gov.au/WebtopEw/ws/samref/sarig1/image/DDD/RB201200012.pdf>.
- Reid, A. J., & Hand, M. (2012). Mesoarchean to Mesoproterozoic evolution of the southern Gawler Craton, South Australia. *Episodes*, 35, 216–225. <https://doi.org/10.18814/epiugs/2012/v35i1/021>
- Reid, A. J., Payne, J. L., & Wade, B. (2006). A new geochronological capability for South Australia: U–Pb dating via LA–ICPMS. *MESA Journal*, 42, 27–31. Department of Primary Industries and Resources South Australia, Adelaide <https://sarigbasis.pir.sa.gov.au/WebtopEw/ws/samref/sarig1/image/DDD/MESAJ042027-031.pdf>.
- Reid, A.J., Tiddy, C., Jagodzinski, E.A., Crowley, J.L., Conor, C., Brotodewo, A. et al. (2021). Precise zircon U–Pb geochronology of hiltaba suite granites, point riley, yorke peninsula. report book 2021/00001, South Australia, Adelaide: Department for Energy and Mining. <https://sarigbasis.pir.sa.gov.au/WebtopEw/ws/samref/sarig1/image/DDD/RB202100001.pdf>.
- Roache, M. W., Allen, S. R., & McPhie, J. (2000). Surface and subsurface facies architecture of a small hydroexplosive, rhyolitic centre in the Mesoproterozoic Gawler Range Volcanics, South Australia. *Journal of Volcanology and Geothermal Research*, 104, 237–259. [https://doi.org/10.1016/S0377-0273\(00\)00208-0](https://doi.org/10.1016/S0377-0273(00)00208-0)
- Schaltegger, U., Schmitt, A. K., & Horstwood, M. S. A. (2015). U–Th–Pb zircon geochronology by ID–TIMS, SIMS, and laser ablation ICP–MS: Recipes, interpretations, and opportunities. *Chemical Geology*, 402, 89–110. <https://doi.org/10.1016/j.chemgeo.2015.02.028>
- Schoene, B., Guex, J., Bartolini, A., Schaltegger, U., & Blackburn, T. J. (2010). Correlating the end-Triassic mass extinction and flood basalt volcanism at the 100 ka level. *Geology*, 38, 387–390. <https://doi.org/10.1130/G30683.1>
- Simpson, C. (2017). Interpretative report on the lower gawler range volcanics in the six mile hill area, report book 2017/00026, South Australia, Adelaide: Department of the Premier and Cabinet. <https://sarigbasis.pir.sa.gov.au/WebtopEw/ws/samref/sarig1/image/DDD/RB201700026.pdf>.
- Skirrow, R.G. (2003). Fe-oxide Cu–Au deposits: Potential of the Curnamona Province in an Australian and global context. Broken hill exploration initiative: Abstracts from the July 2003 conference, Record 2003/13. Geoscience Australia, Canberra, 158–161. https://d28rz98at9flks.cloudfront.net/47786/Rec2003_013.pdf.
- Skirrow, R. G., Bastrakov, E. N., Barovich, K., Fraser, G. L., Creaser, R. A., Fanning, C. M., et al. (2007). Timing of iron oxide Cu–Au–(U) hydrothermal activity and Nd isotope constraints on metal sources in the Gawler Craton, South Australia. *Economic Geology*, 102, 1441–1470, 0361-0128/07/3710/1441-30.
- Sprigg, R. C. (1952). Sedimentation in the Adelaide Geosyncline and the formation of the continental terrace. In M. F. Glaessner, & R. C. Sprigg (Eds.), *Sir douglas mawson anniversary volume* (pp. 153–159). South Australia: The University of Adelaide.
- Stevens, B. P. J., Barnes, R. G., Brown, R. E., Stroud, W. J., & Willis, I. L. (1988). The Willyama Supergroup in the Broken Hill and Euriovie Blocks. *New South Wales. Precambrian Research*, 40–41, 297–327. [https://doi.org/10.1016/0301-9268\(88\)90073-3](https://doi.org/10.1016/0301-9268(88)90073-3)
- Stewart, K. P. (1994). *High temperature volcanism and the role of mantle magmas in proterozoic crustal growth: The Gawler range volcanic province*. Adelaide: University of Adelaide. PhD thesis (unpublished) <https://hdl.handle.net/2440/21477>.
- Szpunar, M., Wade, B., Hand, M. P., & Barovich, K. M. (2007). Timing of proterozoic high-grade metamorphism in the Barossa Complex, southern South Australia: Exploring the extent of the 1590 Ma event. *MESA Journal*, 47, 21–27. <https://sarigbasis.pir.sa.gov.au/WebtopEw/ws/samref/sarig1/image/DDD/MESAJ047021-027.pdf>.
- Tiddy, C. J., & Giles, D. (2020). Suprasubduction zone model for metal endowment at 1.60–1.57 Ga in eastern Australia. *Ore Geology Reviews*, 122, Article 103483. <https://doi.org/10.1016/j.oregeorev.2020.103483>
- Wade, C. E., Payne, J. L., Hill, J., Curtis, S., Barovich, K. M., & Reid, A. J. (2022). Temporal, geochemical and isotopic constraints on plume-driven felsic and mafic components in a Mesoproterozoic flood rhyolite province. *Results in Geochemistry*, 9, 100019.
- Wade, C. E., Reid, A. J., Wingate, M. T. D., Jagodzinski, E. A., & Barovich, K. (2012). Geochemistry and geochronology of the c. 1585 Ma Benagerie Volcanic Suite, southern Australia: relationship to the Gawler Range Volcanics and implications for the petrogenesis of a mesoproterozoic silicic large igneous province. *Precambrian Research*, 206–207, 17–35. <https://doi.org/10.1016/j.precamres.2012.02.020>
- Wade, C. E. (2011). Definition of the mesoproterozoic ninnerie supersuite, Curnamona Province, South Australia. *MESA Journal*, 62, 35–52. <https://sarigbasis.pir.sa.gov.au/WebtopEw/ws/samref/sarig1/image/DDD/MESAJ062025-042.pdf>.
- Werner, M., McAvaney, S.O., Krapf, C.B.E., Pawley, M.J., & Fabris, A.J. (2017). Geology of the peltabinna 1:75 000 map sheet, mineral systems drilling program special map series, report book 2016/00025, South Australia, Adelaide: Department of the Premier and Cabinet. <https://sarigbasis.pir.sa.gov.au/WebtopEw/ws/samref/sarig1/image/DDD/RB201600025.pdf>.